

UNIVERSIDADE FEDERAL DE MINAS GERAIS
Faculdade de Odontologia
Colegiado de Pós-Graduação em Odontologia

Natália Aparecida Gomes

**PARTICIPAÇÃO DE PERICITOS E PROGENITORES NEURAIS NA
ODONTOGÊNESE E ENVELHECIMENTO DENTÁRIO E REPARO
PULPAR APÓS CAPEAMENTO COM MTA ASSOCIADO À
FOTOBIMODULAÇÃO:
*ANÁLISE EM MODELO TRANSGÊNICO IN VIVO NESTIN-GFP/NG2-
DSRED***

**Belo Horizonte
2024**

Natália Aparecida Gomes

**PARTICIPAÇÃO DE PERICITOS E PROGENITORES NEURAIIS NA
ODONTOGÊNESE E ENVELHECIMENTO DENTÁRIO E REPARO
PULPAR APÓS CAPEAMENTO COM MTA ASSOCIADO À
FOTOBIMODULAÇÃO:
*ANÁLISE EM MODELO TRANSGÊNICO IN VIVO NESTIN-GFP/NG2-
DSRED***

Tese apresentada ao Colegiado de Pós-Graduação em Odontologia da Faculdade de Odontologia da Universidade Federal de Minas Gerais para obtenção do título de Doutor - Área de Concentração em Clínica Odontológica.

Orientadora: Profa. Ivana Márcia Alves Diniz

Coorientadora: Profa. Francine Benetti Faria

Coorientador: Prof. Alireza Moshaverinia

Belo Horizonte
2024

Ficha Catalográfica

G633p Gomes, Natália Aparecida.
2024 Participação de pericitos e progenitores neurais na
T odontogênese e envelhecimento dentário, e reparo pulpar após
capeamento com MTA associado à fotobiomodulação: análise em
modelo transgênico in vivo NestinGFP/NG2-DsRed / Natália
Aparecida Gomes. -- 2024.

75 f. : il.

Orientadora: Ivana Márcia Alves Diniz.

Coorientadora: Francine Benetti Faria.

Tese (Doutorado) -- Universidade Federal de Minas
Gerais, Faculdade de Odontologia.

1. Terapia com luz de baixa intensidade. 2. Pericitos.
3. Células-tronco mesenquimais. 4. Polpa dentária. 5.
Materiais biocompatíveis. I. Diniz, Ivana Márcia Alves. II.
Faria, Francine Benetti. III. Universidade Federal de Minas
Gerais. Faculdade de Odontologia. IV. Título.

BLACK - D047



UNIVERSIDADE FEDERAL DE MINAS GERAIS
COLEGIADO DE PÓS-GRADUAÇÃO EM ODONTOLOGIA

ATA DA DEFESA DE TESE DA ALUNA NATÁLIA APARECIDA GOMES

Realizou-se, no dia 24 de outubro de 2024, às 13:30 horas, na sala 3403 da Faculdade de Odontologia da UFMG, da Universidade Federal de Minas Gerais, a defesa de tese, intitulada *ESTUDO SOBRE A FOTOBIMODULAÇÃO DE PERICITOS EM INJÚRIA DA POLPA DENTÁRIA IN VIVO: Uma continuação*, apresentada por NATÁLIA APARECIDA GOMES, número de registro 2020717802, graduada no curso de ODONTOLOGIA, como requisito parcial para a obtenção do grau de Doutor em ODONTOLOGIA, à seguinte Comissão Examinadora: Profa. Francine Benetti - Orientadora (Faculdade de Odontologia da UFMG), Profa. Soraia Macari (Faculdade de Odontologia da UFMG), Profa. Daniela Augusta Barbato Ferreira (UFMG), Profa. Júlia Mourão Braga Diniz (Faculdade Arnaldo), Profa. Renata Gonçalves de Resende (Faculdade Arnaldo).

A Comissão considerou a tese:

Aprovada

Reprovada

Finalizados os trabalhos, lavrei a presente ata que, lida e aprovada, vai assinada por mim e pelos membros da Comissão.

Belo Horizonte, 24 de outubro de 2024.

Profa. Francine Benetti (Doutora)

Profa. Soraia Macari (Doutora)

Profa. Daniela Augusta Barbato Ferreira (Doutor)

Profa. Júlia Mourão Braga Diniz (Doutora)

Profa. Renata Gonçalves de Resende (Doutora)



Documento assinado eletronicamente por **Renata Gonçalves de Resende, Usuário Externo**, em 24/10/2024, às 17:32, conforme horário oficial de Brasília, com fundamento no art. 5º do [Decreto nº 10.543, de 13 de novembro de 2020](#).



Documento assinado eletronicamente por **Júlia Mourão Braga Diniz, Usuária Externa**, em 24/10/2024, às 17:32, conforme horário oficial de Brasília, com fundamento no art. 5º do [Decreto nº 10.543, de 13 de novembro de 2020](#).



Documento assinado eletronicamente por **Francine Benetti, Professora do Magistério Superior**, em 24/10/2024, às 17:50, conforme horário oficial de Brasília, com fundamento no art. 5º do [Decreto nº 10.543, de 13 de novembro de 2020](#).



Documento assinado eletronicamente por **Daniela Augusta Barbato Ferreira, Usuária Externa**, em 24/10/2024, às 18:00, conforme horário oficial de Brasília, com fundamento no art. 5º do [Decreto nº 10.543, de 13 de novembro de 2020](#).



Documento assinado eletronicamente por **Soraia Macari, Professora do Magistério Superior**, em 24/10/2024, às 18:11, conforme horário oficial de Brasília, com fundamento no art. 5º do [Decreto nº 10.543, de 13 de novembro de 2020](#).



A autenticidade deste documento pode ser conferida no site https://sei.ufmg.br/sei/controlador_externo.php?acao=documento_conferir&id_orgao_acesso_externo=0, informando o código verificador **3604264** e o código CRC **1FED4CC6**.

AGRADECIMENTOS

A Deus,

Obrigada por me guiar durante a realização deste projeto. Principalmente por iluminar cada escolha e colocar inúmeros obstáculos no meio do caminho, para que eu percebesse que estava sob Seu controle. Creio que Ele trouxe este doutorado como uma missão de vida, de crescimento pessoal e intelectual com pessoas e circunstâncias inimagináveis que venci por estar sob Suas mãos.

Aos meus pais Valdir e Valdirene,

Por me ensinarem a lutar pela vida e pelos meus objetivos de forma honesta, com as pessoas e comigo mesma. Pai, obrigada por mesmo sem entender os meus sonhos, apoiá-los e vibrar a cada conquista e passo dado em direção a concretização deles. Mãe, obrigada por me proteger, amparar e me mostrar o valor do autocuidado em forma de amor e carinho para facilitar a passagem pelos processos. Obrigada por estarem ao meu lado e confiarem em mim. Vocês são o sentido da minha vida.

Aos meus irmãos Lucas, Matheus e Talita,

Por todo o companheirismo e por me mostrarem que somos melhores ao lado de pessoas que nos amam. Luquinhas obrigada por ser um menino gentil e nunca questionar minhas ausências desde que saí muito cedo de nossa casa para estudar, você ainda era um bebê muito amoroso e hoje, é um rapaz inteligente e atento às coisas ao seu redor, Matheus meu querido irmão, obrigada por ser meus ouvidos sem julgamentos e meu ponto de reflexão. Talita, quanto orgulho eu sinto, da mulher incrível que se tornou e obrigada por me permitir experimentar o amor mais puro que já senti me fazendo tia desse ser maravilhoso, nossa amada Letícia. Vocês foram meu suporte emocional, minha base e minha fortaleza.

À professora Ivana Márcia Alves Diniz,

Pelo seu tempo! Querida orientadora, agradeço por me ensinar tanto, por ser além do que se propôs, por ser professora, por ser ouvidos, por ser casa, por ser

aprendizado contínuo, dedicação e perseverança. Obrigada por me despertar reflexões, por ser honesta e compartilhar sua experiência de vida e de trabalho comigo. Serei eternamente grata a todo o processo de construção que foram todos esses nossos anos de trabalho juntas.

À professora Francine Benetti,

Pela orientação, por compartilhar seu conhecimento de uma forma serena, cuidadosa e respeitosa. Obrigada por me ensinar a ter calma diante das turbulências e sempre contribuir através de palavras sábias e em momentos oportunos.

Ao meu amado grupo de pesquisa,

Pela amizade, pela cooperação, pelo respeito. Agradeço especialmente, Luiza minha eterna sister você foi muito mais que uma colega durante todo esse tempo, cafés no ICB contaram histórias para meus netos, pode ter certeza! Luri, meu querido amigo que me acompanha desde o início dessa caminhada, sempre com um sorriso no rosto e compartilhando suas vivências com uma lealdade admirável, obrigada por estar ao meu lado sempre. Humberto um menino de história inspiradora, de um sarcasmo que tornavam as tardes no biotério agradáveis, obrigada por segurar várias barras comigo. Rafaela, sonhadora, dedicada, meu orgulho que nesse momento voou para o mundo atrás de seus sonhos, obrigada por me apoiar sempre. Aos meus queridos amigos do ICB Pedro Prazeres e Walisson que me ensinaram sobre experimentação animal, Caroline Piccoli sobre confocal e Aline. Aos meus amados ICs, João, Felipe, Beatriz, Luiza Diniz, Talyta e Ana Luiza, obrigada por tudo sempre, vocês foram essenciais. Sem a contribuição de cada um esse trabalho não seria possível e a caminhada não seria tão boa.

Aos demais professores,

Em especial aos professores Ricardo Mesquita, Gerluza Borges e Gleide Amaral pela colaboração com a pesquisa originada deste mestrado. Aos professores Flávio Almeida Amaral, Alexander Birbrair e pela disponibilidade de suas instalações e equipamentos para execução do estudo. Agradeço também aos professores do programa de Clínica Odontológica, em especial aos professores Allyson Moreira, Cláudia Silami, Soraia Macari: o meu agradecimento pelos ensinamentos

transmitidos.

Aos amigos da pós-graduação e da pesquisa,

Em especial Natália, Richard, Tânia, Isadora, e Bruno. Poder contar com vocês durante esta caminhada foi essencial para que crescêssemos juntos e especialmente aliviar nossas apreensões durante esses dois anos. Obrigada por fazerem parte dessa fase especial.

À equipe de apoio,

Especialmente Mara, Domênico e a Daniela por colaborarem com a construção desse trabalho de forma singular dispondo de seus conhecimentos e técnicas para que essa pesquisa fosse realizada.

À melhor família e aos amigos,

Obrigada por apoiar, incentivar e torcer por essa conquista. Agradeço também por compreenderem minha ausência e mesmo assim tornarem-se presentes. Obrigada por cada palavra de conforto, orações e pelo carinho ao longo dessa trajetória.

Ao meu companheiro Daniel,

Obrigada por ser um companheiro incrível, por cada palavra de incentivo e confiança, pelas tentativas de distração em momentos difíceis, pela paciência, pelo amor e por ser meu porto seguro.

Ao Colegiado de Pós-Graduação,

Pós-Graduação da Faculdade de Odontologia da Universidade Federal de Minas Gerais, na pessoa da coordenadora, Professor Mauro de Abreu, pela condução do nosso programa de excelência; também a sua secretaria e agências de apoio.

Às agências de fomento,

CAPES, CNPq e FAPEMIG pelo apoio institucional ao Programa de Pós-Graduação da UFMG .

“Não nascemos prontos, nós nos preparamos pelo caminho.”

Mário Sérgio Cortella

RESUMO

Pericitos e células neurais são conhecidos por colaborar na regeneração do tecido pulpar. Terapias celulares capazes de estimular esses componentes podem ter relevância terapêutica em condições de polpa dental vital. O objetivo desse estudo foi mapear progenitores neurais e pericitos durante a odontogênese e envelhecimento dentário e comparar a ação dessas células no dente adulto após o capeamento pulpar com Agregado Trióxido Mineral (MTA) e MTA associado à fotobiomodulação (PBMT), após 07 e 21 dias. Foram utilizados animais C57BL/6 transgênicos duplos positivos NestinGFP/NG2DsRed para o rastreamento dessas células, sendo a Nestina um marcador de progenitores neurais indiferenciados e a proteína NG2 um marcador de pericitos. Duas subpopulações de pericitos foram também investigadas, aquelas Nestina+NG2+ e aquelas Nestina-NG2+. Dentes de animais neonatos de 1 e 14 dias que não sobreviveram à vida adulta e de animais adultos de 2 e 12 meses, foram analisados para a compreensão da participação das células marcadas durante a odontogênese e envelhecimento dentário. Em seguida, animais adultos (2 meses) passaram por uma injúria experimental na polpa dentária do seu primeiro molar superior. As cavidades foram tratadas com MTA ou MTA associado à PBMT (5 J/cm², 7s, 20 mW, 0,71W/cm²) diariamente nos tempos de 0, 24, 48 e 72 horas. As cavidades foram então seladas com resina fluida fotoativada e os animais eutanasiados nos tempos 7 e 21 dias. O rastreamento celular foi feito por microscopia confocal, onde os canais verde (GFP), vermelho (DsRed), azul (Dapi) e suas composições foram utilizados para quantificar a fluorescência celular no tecido. Arquitetura tecidual foi avaliada por histologia de rotina para avaliar os sinais de vitalidade pulpar, presença de vasos sanguíneos e sinais inflamatórios, enquanto a presença de dentina ou osteodentina, nódulos e calcificações difusas foi observada por meio do Tricrômico de Masson. Genes relacionados às células de interesse (*Nestin*, *NG2*, *GFAP*), ao reparo tecidual (*CXCL12*, *CD105*) e odontogênese (*RUNX-2* e *DSPP*) foram quantificados por RT-qPCR. Demonstramos que os pericitos parecem ser células progenitoras para odontoblastos durante a odontogênese e que a proteína NG2 é reexpressa em dentes que sofreram algum tipo de estímulo nocivo ao longo da vida. Os dentes constituem fontes de células progenitoras neurais, mesmo em animais com 12 meses de idade. Após o capeamento pulpar com MTA, a PBMT como tratamento adjuvante promoveu reparo mais semelhante ao tecido pulpar original, com menos sinais inflamatórios e qualitativamente menos calcificações pulpares. Após 21 dias, a população de células positivas para os marcadores de indiferenciação *Nestin* e *GFAP* foi maior que o grupo controle. A associação entre MTA e PBMT levou à formação de dentina com expressão significativa de *DSPP* e *RUNX-2* comparado ao grupo tratado exclusivamente com MTA. A associação MTA/PBMT parece ser promissora para o tratamento conservador da polpa dentária.

Palavras-chave: fotobiomodulação; pericitos; células-tronco mesenquimais; polpa dentária; agregado trióxido mineral; biomateriais; odontogênese.

ABSTRACT

Participation of pericytes and neural progenitors in odontogenesis and dental aging, and pulp repair after capping with MTA associated with photobiomodulation: *in vivo* analysis in transgenic NESTIN-GFP/NG2-DSRED model

Pericytes and neural cells are known to collaborate in the regeneration of pulp tissue. Cell-based therapies that can stimulate these components may hold therapeutic relevance in vital dental pulp conditions. The objective of this study was to map neural progenitors and pericytes during odontogenesis and dental aging, and to compare the actions of these cells in adult teeth following pulp capping with Mineral Trioxide Aggregate (MTA) and MTA in conjunction with photobiomodulation (PBMT) after 7 and 21 days. Transgenic double-positive NestinGFP/NG2DsRed C57BL/6 mice were utilized for tracking these cells, with Nestin serving as a marker for undifferentiated neural progenitors and the NG2 protein as a marker for pericytes. Two subpopulations of pericytes were also investigated: those that were Nestin+NG2+ and those that were Nestin-NG2+. Teeth from neonatal animals at 1 and 14 days, which did not survive to adulthood, as well as from adult animals aged 2 and 12 months, were analyzed to understand the role of the marked cells during odontogenesis and aging. Subsequently, adult animals (2 months) underwent experimental injury to the dental pulp of their first upper molars. The cavities were treated with either MTA or MTA combined with PBMT (5 J/cm², 7s, 20 mW, 0.71 W/cm²) daily at time points of 0, 24, 48, and 72 hours. The cavities were then sealed with photoactivated flow resin, and the animals were euthanized at 7 and 21 days. Cellular tracking was performed using confocal microscopy, where the green (GFP), red (DSRed), and blue (DAPI) channels and their compositions were utilized to quantify cellular fluorescence in the tissue. Tissue architecture was assessed through routine histology to evaluate signs of pulp vitality, presence of blood vessels, and inflammatory markers, while the presence of dentin or osteodentin, nodules, and diffuse calcifications was observed using Masson's trichrome staining. Genes related to the cells of interest (Nestin, NG2, GFAP), tissue repair (CXCL12, CD105), and odontogenesis (RUNX-2 and DSPP) were quantified via RT-qPCR. We demonstrated that pericytes appear to serve as progenitor cells for odontoblasts during odontogenesis, and that the NG2 protein is re-expressed in teeth that have undergone some form of harmful stimulus throughout their lifespan. Teeth constitute sources of neural progenitor cells, even in animals aged 12 months. Following pulp capping with MTA, PBMT as an adjunct treatment promoted repair that resembled original pulp tissue more closely, with fewer inflammatory signs and qualitatively reduced pulp calcifications. After 21 days, the population of cells positive for the undifferentiated markers Nestin and GFAP was greater than that in the control group. The combination of MTA and PBMT resulted in significant dentin formation with notable expression of DSPP and RUNX-2 compared to the group treated exclusively with MTA. The MTA/PBMT combination appears promising for the conservative treatment of dental pulp.

Keywords: photobiomodulation; pericytes; mesenchymal stem cells; dental pulp; mineral trioxide aggregate; biomaterials; odontogenesis.

LISTA DE FIGURAS

Figura 1	Mesa cirúrgica personalizada confeccionada através da impressão 3D.	23
Figura 2	Primeiro passo na realização da injúria pulpar aspecto extraoral	23
Figura 3	Remoção superficial do esmalte com broca LN, seguido pela remoção da dentina com lima endodôntica até o teto da cavidade pulpar	24
Figura 4	Aspecto final da injúria realizada efetivamente, seguida de magnificação com câmera intraora	24
Figura 5	Aspecto final da injúria tratada com MTA, seguida de restauração com resina fluida	25

Figuras Artigo 1

Figure 1	<i>Labelled Cells Characterization in Postnatal Odontogenesis</i>	33
Figure 2	<i>Characterization of cells after mantle dentin production in odontogenesis</i>	34
Figure 3	<i>Characterization of cells after mantle dentin production in odontogenesis</i>	35
Figure 4	<i>Demonstration of the same tooth at different cutting depths</i>	36
Figure 5	<i>Characterization of Nestin and NG2 cells in young adult teeth</i>	37
Figure 6	<i>Characterization of cells after natural occlusal wear in mature teeth</i>	38

Figuras Artigo 2

Figure 1	<i>Analysis of pericytes and neural cells in healthy tissues and after injury treated with MTA and MTA+PBMT for 7 days</i>	53
Figure 2	<i>Analysis of pericytes and neural cells in healthy tissues and after injury treated with MTA and MTA+PBMT for 21 days</i>	54
Figure 3	<i>Analysis of mineralization in dental pulp after capping with MTA or photoactivated MTA after 7 days – Masson's Trichrome</i>	55

- Figure 4 *Analysis of mineralization in dental pulp after capping with MTA or photoactivated MTA after 21 days – Masson’s Trichrome* 56
- Figure 5 *Analysis of inflammatory signs after treatment with MTA and photoactivated MTA in 7 days – Hematoxilin and Eosin* 57
- Figure 6 *Analysis of inflammatory signs after treatment with MTA and photoactivated MTA in 21 days – Hematoxilin and Eosin* 58

LISTA DE TABELAS

TABELA 1 Sequência de primers utilizados para análise qPCR

26

LISTA DE ABREVIATURAS E SIGLAS

α SMA	Alfa-Actina de Músculo Liso (<i>A-Smooth Muscle Actin</i>)
Bsp	Sialoproteína Óssea (<i>Bone Sialoprotein</i>)
Ca(OH) ₂	Hidróxido de Cálcio
CD105	Endoglina
CEUA	Comissão de Ética no Uso De Animais
CV	Coeficiente de Variação
CXCI-12	<i>C-X-C Motif Chemokine Ligand 1</i>
DAPI	<i>4',6'-Diamino-2-Fenil-Indol</i>
DPC	Células da Polpa Dentária
DsRed	Proteína Vermelha Fluorescente (<i>Red Fluorescent Protein</i>)
Dspp	Sialoproteína Fosfodentinária (<i>Dentin Sialophosphoprotein</i>)
DSPCs	Células-Tronco da Polpa Dentária (<i>Dental Pulp Stem Cells</i>)
FGF	Fator de Crescimento de Fibroblastos (Fibroblast Growth Factor)
GAPDH	Gliceraldeído-3-Fosfato Desidrogenase (<i>Glyceraldehyde-3-Phosphate Dehydrogenase</i>)
GFAP	Proteína Glial Ácida Fibrilar (<i>Glial Fibrillary Acidic Protein</i>)
GFP	Proteína Verde Fluorescente (<i>Green Fluorescent Protein</i>)
H&E	Hematoxilina e Eosina
IC	Intervalo de Confiança
InGaAlP	Fosforeto de Índio-Gálio-Alumínio (<i>Indium-Gallium-Aluminum-Phosphide</i>)
MTA	Agregado Trióxido Mineral (<i>Mineral Trioxide Aggregate</i>)
MSCs	Células-Tronco Mesenquimais (<i>Mesenchymal Stem Cells</i>)
NG2	Antígeno Neural/Glial 2 (<i>Neural/Glial Antigen 2</i>)
OCT	Optimum Cutting Temperature
PBMT	Terapia por Fotobiomodulação (<i>Photobiomodulation</i>)
PBS	Tampão Fosfato-Salino (<i>Phosphate Buphered Saline</i>)
PDGFR- β	Receptor Beta do Fator de Crescimento Derivado de

	Plaquetas (<i>Platelet-derived Growth Factor Receptor-β</i>)
PFA	Paraformaldeído
RUNX-2	Fator de Transcrição Relacionado ao Runt 2 (<i>Runt-Related Transcription Factor 2</i>)
TM	Tricrômico de Masson
TGF-β1	Fator de Crescimento Transformante (<i>Transforming Growth Factor</i>)-β1
SDF1- α	<i>Stromal Cell-Derived Factor 1-alpha</i>
Twist	<i>Twist-Related Protein 1</i>
P38	<i>P38 Mitogen-Activated Protein Kinase (MAPK)</i>

SUMÁRIO

1 CONSIDERAÇÕES INICIAIS	15
2 OBJETIVOS	20
2.1 Objetivos Geral	20
2.2 Objetivos Específicos	20
3 METODOLOGIA EXPANDIDA	21
3.1 Aspectos éticos	21
3.2 Expansão das colônias de Nestina GFP/NG2 DsRed	21
3.3 Ensaio <i>in vivo</i>	22
3.3.1 Parte I - Caracterização de Células NG2+, Nestin+ e Nestin+NG2+ durante a odontogênese e envelhecimento dentário	22
3.3.1.2 Microscopia confocal	22
3.3.2.1 Parte II - Injúria experimental na polpa dentária de camundongos adultos tratados MTA associado à fotobiomodulação ou não	23
3.3.2.2 Análises em RT-qPCR	27
3.3.2.3 Análises Histológicas	28
3.3.2.4 Microscopia confocal	28
3.3.2.5 Histologia (H&E e Tricômio de Masson)	28
3.3.2.6 Análise Estatística	29
4 RESULTADOS	30
4.1 Artigo 1 - Mapping pericytes and neural progenitors' temporo-spatial distribution during postnatal odontogenesis and dental aging in Nestin+NG2+transgenic mice	30
4.2 Artigo 2 - Mastering dentinogenesis using adjuvant photobiomodulation therapy in murine conservative dental pulp procedures	47
5 CONSIDERAÇÕES FINAIS	71
REFERÊNCIAS	72
ANEXO	75

1 CONSIDERAÇÕES INICIAIS

Terapias baseadas em células-tronco da polpa dentária (DPSCs, do inglês *Dental Pulp Stem Cells*) estão emergindo rapidamente como tratamentos conservadores capazes de induzir a regeneração do tecido pulpar. O objetivo destes tratamentos é restabelecer aspectos funcionais e fisiológicos semelhantes ao tecido pulpar original, garantindo, dentre outras características, a manutenção da propriedade sensorial do elemento dentário. No entanto, as dificuldades de expansão de células-tronco *in vitro* e incompatibilidades imunológicas entre diferentes doadores limitam o uso de abordagens que utilizam DPSCs transplantadas como forma de tratamento. Nesse sentido, é ideal que sejam aprimoradas as ferramentas capazes de estimular as células-tronco mesenquimais (MSCs, do inglês *Mesenchymal Stem Cells*) endógenas a regenerar tecidos parcialmente perdidos, como a polpa dentária.

O tecido pulpar é altamente vascularizado e rico em células de origem neural, células indiferenciadas e pericitos. Os pericitos, as quais dividem sua localização com células endoteliais nos vasos sanguíneos, são semelhantes aos progenitores de MSCs e possuem alto potencial de diferenciação dependendo do grau de comprometimento de suas subpopulações, sendo capazes de gerar células adipogênicas, fibrogênicas, musculares, angiogênicas e neurogênicas (BIRBRAIR *et al.*, 2013, 2015; GOMES *et al.*, 2022; YANNI e SHARPE, 2019). Dessa forma, pericitos que expressam simultaneamente as proteínas Nestina e NG2 são considerados mais plásticos e chamados pericitos tipo II, enquanto aqueles que expressam exclusivamente a proteína NG2 são chamados de pericitos tipo I (BIRBRAIR *et al.*, 2013; GOMES *et al.*, 2022).

Diversas evidências científicas reforçam o papel dos pericitos como células-tronco multipotentes, pois demonstraram sua contribuição para a formação de diferentes tecidos (ALLIOT-LICHT *et al.*, 2001; CAPLAN, 2008; CRISAN *et al.*, 2008; DELLAVALLE *et al.*, 2007; DORE-DUFFY *et al.*, 2011; FENG *et al.*, 2011; SHI, GRONTHOS, 2003).

Além disso, estudos sugerem que pericitos possuem funções reguladoras, imunológicas e fagocíticas, bem como um papel importante na homeostase tecidual (BIRBRAIR *et al.*, 2017). Essas células podem ser mais bem identificadas por sua localização perivascular (ZIMMERMANN, 1923) e marcadores moleculares – como *neural/glial antigen 2* (NG2), *Platelet Derived Growth Factor Receptor-β* (PDGFR-β),

e α -Smooth Muscle Actin (α -SMA) (FENG *et al.*, 2011; SA-PEREIRA *et al.*, 2012). Seu fenótipo pode ser impreciso, uma vez que possuem grande heterogeneidade dependendo das estruturas e órgãos em que são investigados (SHI, GRONTHOS, 2003; YANNI, SHARPE, 2019).

Em 2003, um estudo sugeriu que a origem das DPSCs seria perivascular (SHI, GRONTHOS, 2003). Posteriormente, Løvschall *et al.* (2007) conseguiram verificar a presença de pericitos na polpa dentária através de um estudo sobre a formação de dentes em roedores e análise de dentes injuriados humanos. No entanto, somente em 2011, Feng *et al.* (2011) demonstraram, por meio de um modelo de rastreamento genético – LacZ, a presença de pericitos no plexo vascular de incisivos de camundongos e sua participação direta em situações de injúria da polpa dentária. Foi visto que um pequeno número de pericitos (em torno de 10% das células) povoa o mesênquima dentário durante o desenvolvimento, onde eles permanecem essencialmente quiescentes até ocorrerem danos à camada odontoblástica. Na presença de dano, há estímulos à proliferação desses pericitos, os quais aumentam em número e efetivamente contribuem para a formação de novos odontoblastos (FENG *et al.*, 2011). Por outro lado, os autores também identificaram que os pericitos contribuem apenas com um pequeno percentual desses novos odontoblastos, sugerindo que a reposição dessas células também pode ser mobilizada de outras fontes (FENG *et al.*, 2011).

Mais tarde, em 2014, um estudo publicado na *Nature* demonstrou que as células de Schwann e/ou seus precursores, oriundas do sistema nervoso periférico, dariam de fato origem à maior parte das MSCs da polpa dentária e dos odontoblastos em dentes adultos (KAUKUA *et al.*, 2014). Na verdade, as células de Schwann e seus precursores seriam células da crista neural dormentes, as quais poderiam ser recrutadas dos nervos contribuindo para a manutenção dos tecidos periféricos (KAUKUA *et al.*, 2014). Nesse mesmo estudo, os pericitos foram excluídos como intermediários para as MSCs da polpa e odontoblastos derivados de células de Schwann e/ou seus precursores, sugerindo que eles seriam uma fonte adicional e independente de células indiferenciadas capazes de repor odontoblastos perdidos.

Nosso grupo de pesquisa demonstrou, ainda que preliminarmente, que a polpa dentária pode ser regenerada por meio do procedimento endodôntico regenerativo, seguido da terapia por fotobiomodulação (PBMT, do inglês *Photobiomodulation therapy*) com laser vermelho (660 nm). Nesse estudo, ratos tiveram a remoção completa

do tecido pulpar e em seguida foi realizado um tratamento com solução ácida para liberação de fatores de crescimento das paredes dentinárias do canal radicular, e indução de sangramento intracanal para formação de um coágulo sanguíneo, previamente à aplicação da fotobiomodulação. Após 4 semanas, um tecido neoformado similar ao tecido original da polpa dentária foi observado (MOREIRA *et al.*, 2017).

A PBMT é uma terapia que utiliza de fontes de luz não ionizantes, especificamente a luz vermelha com comprimento de onda de 660nm, tem sido amplamente investigada por seu potencial em aliviar a dor, modular processos inflamatórios e imunológicos, além de estimular a reparação e regeneração tecidual (GARCEZ *et al.*, 2012). No complexo dentino-pulpar, a fotobiomodulação demonstrou eficácia na indução de diferenciação de células-tronco em odontoblastos, promovendo a dentinogênese (ARANI *et al.*, 2014). Adicionalmente, foi associada à formação de tecido funcionalmente semelhante à polpa dentária, com vascularização e inervação, após procedimento endodôntico regenerativo (MOREIRA *et al.*, 2017).

A fim de identificar alguns protagonistas celulares envolvidos nesta regeneração, realizamos um estudo de curto prazo de observação utilizando o modelo de exposição pulpar artificial em camundongo transgênico Nestina GFP/NG2 DsRed, o qual é representativo das populações celulares multipotentes na polpa dentária (GOMES *et al.*, 2022). Neste modelo, rastreamos e analisamos o comportamento de células indiferenciadas ou progenitores de origem neural que expressam nestina (os quais podem compreender a população de células de Schwann e seus precursores) e pericitos – via expressão de NG2. Neste estudo, após 3 dias de fotobiomodulação, foi observado que a PBMT promoveu um aumento no número total de células, mas particularmente de pericitos em torno do tecido pulpar danificado (GOMES *et al.*, 2022). Neste estudo, a fotobiomodulação foi capaz de estimular a microvasculatura local de modo a manter a vitalidade da polpa coronária, ainda que qualquer tipo de restauração ou material bioativo não tenha sido realizada.

No caso de exposições pulpares acidentais ou por lesões cariosas, dependendo do diagnóstico pulpar, tratamentos conservadores são preferíveis em relação aos tratamentos endodônticos radicais (ZANINI; MEYER; SIMON, 2017). No caso de exposições de pequena extensão, os capeamentos diretos são uma opção terapêutica com taxa de sucesso de 74% a 96% (CUSHLEY *et al.*, 2021). Nos casos de comprometimento pulpar de maior magnitude, as pulpotomias são consideradas.

Nesse sentido, tecido pulpar ainda vital ou parcialmente vital parecem ser capazes de reestabelecer a homeostase do complexo dentino-pulpar (ALQADERI *et al.*, 2016; CUSHLEY *et al.*, 2019; ELMSMARI *et al.*, 2019). Os tratamentos utilizados nos tratamentos regenerativos da polpa (TRP) envolvem, de forma genérica, o uso de biomateriais como o hidróxido de cálcio (Ca(OH)₂) e o agregado trióxido mineral (MTA, do inglês *Mineral Trioxide Aggregate*). Esses materiais têm demonstrado a indução da formação de ponte reparadora de dentina e preservação da vitalidade pulpar. O Ca(OH)₂ apresenta características antibacterianas e promove a formação de dentina terciária, porém sua capacidade de vedamento e a qualidade dessa dentina neoformada têm sido questionadas (DIDILESCU *et al.*, 2018). Cimentos à base de silicato de cálcio, como o MTA, têm sido indicados como potenciais materiais para capeamento pulpar por apresentarem biocompatibilidade, excelente bioatividade, boa capacidade de vedamento e indução de barreira dentinária consistente (DAVAIE *et al.*, 2021; UTNEJA *et al.*, 2015). Cimentos à base de silicato de cálcio são padrão ouro para tratamentos conservadores da polpa dentária atualmente, entretanto, apresentam alto custo e dificuldade de manipulação. Novas tecnologias podem ser incorporadas ou otimizadas para reduzir o custo e tempo dos tratamentos, além de melhorar o prognóstico de dentes tratados com terapias conservadoras pulpares.

Outra alternativa terapêutica que tem sido utilizada com sucesso na modulação de processos inflamatórios, analgesia e cicatrização/reparo tecidual em vários órgãos é a PBMT, e de acordo com o descrito anteriormente, pode ser no futuro uma ferramenta poderosa na engenharia tecidual (OLIVEIRA *et al.*, 2022; VALLE *et al.*, 2020). É possível que pericitos constituam parte das MSCs endógenas que repovoam o canal radicular quando estimulados pela PBMT, embora nossos estudos preliminares tenham sido insuficientes para comprovar isso. Previamente, Arany *et al.* (2014) demonstraram que a PBMT pode estimular a formação de dentina terciária através da via de ativação de TGF (*Transforming Growth Factor-β1*). Resta saber qual a contribuição dos pericitos e suas subpopulações para a formação deste tecido mineralizado. Mais que isso, ainda se conhece pouco os efeitos da PBMT quando associados a materiais capeadores diretos.

Assim, o objetivo deste estudo foi avaliar a capacidade estimuladora da PBMT na modulação de pericitos e outras populações indiferenciadas no reparo da polpa dentária após injúria tecidual e capeamento pulpar com MTA. Além disso, propusemos

um estudo preliminar para caracterizar essas células durante a odontogênese e envelhecimento dentário. Para estes fins, foi utilizado um modelo de camundongo (C57BL/6) transgênico Nestina GFP/NG2 DsRed com marcadores fluorescentes específicos, ou repórteres, para as proteínas nestina e NG2, o qual permitiu mapear a localização e a ação de células progenitoras neurais (Nestina+) e pericitos (NG2+) sob a estimulação dos tratamentos ao longo do tempo.

2. OBJETIVOS

- Objetivo Geral

O objetivo desse estudo foi analisar células NG2+, Nestin+ e Nestin+NG2+ durante a odontogênese e envelhecimento dentário, além de comparar a distribuição e ação destas células após o capeamento pulpar de primeiros molares com o MTA associado ou não à fotobiomodulação (PBMT).

- Objetivos Específicos

- Localizar as células NG2+, Nestin+ e Nestin+NG2+ durante a odontogênese nos tempos de 1 dia, 14 dias, 2 meses e 12 meses, através da microscopia confocal;
- Avaliar e comparar a mobilização de células NG2+, Nestin+ e Nestin+NG2+ após 7 e 21 dias das exposições pulpares nos grupos MTA e MTA/PBMT, por microscopia confocal;
- Graduar o processo inflamatório induzido na polpa dentária desses grupos após 7 e 21 dias das exposições pulpares, através da análise histológica;
- Comparar qualitativamente a produção de dentina terciária, formação de nódulos mineralizados e calcificações difusas, nos dentes tratados com os materiais supracitados após 7 e 21 dias, por meio da análise histológica através da coloração de Tricômio de Masson;
- Avaliar a expressão dos genes NG2 (Proteoglicano 4 de Sulfato de Controitina), Nestin, GFAP (Proteína Glial Ácida Fibrilar), SDF1- α (Stromal Cell-Derived Factor 1-alpha), Twist-2 (Twist-related Protein 1), P38 (p38 Mitogen-Activated Protein Kinase (MAPK) nos dentes tratados com MTA fotoativado ou não, após 07 dias;
- Avaliar a expressão dos genes NG2 (Proteoglicano 4 de Sulfato de Controitina), Nestin, GFAP (Proteína Glial Ácida Fibrilar), DSPP (Sialofosfoproteína da Dentina), RUNX-2 (Fator de Transcrição 2 da Família RUNT), CD105 (Endoglina) nos dentes tratados com MTA fotoativado ou não, após 21 dias.

3 METODOLOGIA EXPANDIDA

3.1 Aspectos éticos

Este estudo foi submetido e aprovado pelo Comitê de Ética de Pesquisa em Animais da Universidade Federal de Minas Gerais (CEUA: 181/2020). Para o cálculo da quantidade de animais, foi utilizada uma das variáveis mais instáveis correspondente aos pericitos, o PDGFR- β , com coeficiente de variação de 23% (KYYRIAINEN *et al.*, 2017). Para a garantia de uma viabilidade experimental segura, consideramos um intervalo de confiança de 20% - dentro do limite de 30% e adequado ao coeficiente de variação da variável (SAMPAIO, 2007). De acordo com Sampaio, 2007, $CV = IC.2/\sqrt{n}$.

Em que,

CV = coeficiente de variação;

IC = intervalo de confiança;

N = número de camundongos por grupo. Substituindo os valores das incógnitas:

$$n = (2XCV)^2/IC^2$$

$$n = (2X23)^2/20^2$$

$$n = 2116/400$$

$$n = 5,29$$

Arredondando o n encontrado para um valor inteiro, temos $n = 6$ para o experimento *in vivo*.

3.2 Expansão das colônias de Nestina GFP/NG2 DsRed

Os animais transgênicos com o fenótipo esperado Nestin GFP/NG2 DsRed foram obtidos pelo cruzamento de machos Nestin GFP+ com fêmeas Nestin GFP+/NG2 DsRed+. Os animais homozigotos positivos para um dos genes foram usados em outros cruzamentos. Os animais duplo-positivos foram os de interesse nesse estudo.

Os animais que compuseram os experimentos de caracterização durante a odontogênese e envelhecimento dentário foram aqueles que seriam descartados por causas naturais. Os animais neonatos que foram rejeitados pelas fêmeas após o nascimento com idades de 1 e 14 dias foram coletados, e animais que não se

encontravam em idade reprodutiva, possuindo mais de 10 meses de idade.

3.3 Ensaios *in vivo*

3.3.1 Parte I - Caracterização de Células NG2+, Nestin+ e Nestin+NG2+ durante a odontogênese e envelhecimento dentário

Para obtenção dos filhotes neonatos de 1 ou 14 dias de vida, as matrizes utilizadas na expansão da colônia Nestin GFP+/NG2 DsRed+ foram observadas durante o seu período reprodutivo. Foi observada a inviabilidade de filhotes no ninho, seja por traumas por pisoteamento dos animais adultos ou morte iminente por qualquer outro motivo. Animais nessas condições foram coletados para que fases diferentes da odontogênese pós-natal pudessem ser analisadas. Matrizes fêmeas com 12 meses de idade, ou seja, fora de sua atividade reprodutiva, também foram coletados para que os dentes fossem observados após o envelhecimento natural, sem a indução de estímulos externos. Nesses animais nenhuma intervenção foi realizada. Os animais foram eutanasiados com sobredose anestésica (300 mg/Kg de Cetamina e 30 mg/Kg de Xilazina, via intraperitoneal), seguida de deslocamento cervical para certificação.

As maxilas e mandíbulas foram removidas e fixadas em solução de paraformaldeído (PFA) à 4%, durante 24 horas. Em seguida, foram lavadas em solução salina de tampão fosfato (PBS) e desmineralizados em EDTA 10% durante um período de 28 dias, com exceção dos espécimes de neonatos de 1 dia, que dispensaram a desmineralização. Por fim, foram preparados para análise histológica como descrito abaixo.

3.3.1.2 Microscopia confocal

Os espécimes depois de fixados e desmineralizados como descrito anteriormente na seção de ensaios *in vivo*, foram crioprotetidos com Sacarose 30% overnight e embidos em meio de inclusão Optimum Cutting Temperature OCT. Seções de 25 µm de espessura foram cortadas em criostato e montadas em lâminas de vidro.

Os cortes foram contra-corados com DAPI em meio de montagem (Abcam, Cambridge, EUA). Foram utilizadas as objetivas Plan Apo 20x e 40x. As células

indiferenciadas marcadas pela fluorescência endógena visualizada em verde (GFP), a população total de pericitos por marcação endógena vermelha (DsRed) e as subpopulações de pericitos Tipo 1 (colocalização de marcadores DsRed e DAPI em rosa) e Tipo 2 (colocalização de GFP, DsRed e DAPI em amarelo) foram analisadas em software Fiji (NIH, Bethesda, EUA).

Imagens foram obtidas das estruturas que correspondiam ao período de formação dentária. No período de 1D, imagens padronizadas com a visualização completa do germe dentário e aumento de 20x em estruturas específicas como o folículo dental, retículo estrelado, estrato intermediário e papila dental para que pudessem ser observadas. No período de 14 dias, o folículo dental, dentina e polpa dental foram analisadas no mesmo aumento. No período de 2 meses, os três cornos pulpares precisavam ser observados em sua totalidade e as raízes mesial e distal em sua completude, o mesmo foi observado para a obtenção das imagens dos dentes de animais com 12 meses de idade no aumento de 20x e 40x.

3.3.2.1 Parte II - Injúria experimental na polpa dentária de camundongos adultos tratados MTA associado à fotobiomodulação ou não

Os camundongos foram anestesiados (100 mg/Kg de Cetamina e 10 mg/Kg de Xilazina, via intraperitoneal) e posicionados em mesa cirúrgica confeccionada por impressora tridimensional (3D) em filamento de nylon 12 (3D Fortus 380 MC, Stratasys, EUA), com design de suporte de cabeça (adaptado de MARCHESAN *et al.*, 2018) para permitir o acesso intrabucal (Figura 1 e 2). Resumidamente, foi realizada exposição pulpar na fossa mesial do primeiro molar superior esquerdo de camundongos Nestin GFP+/NG2 DsRed+ ou WT com dois meses de idade. Para tanto, com o auxílio de broca esférica LN (Maillefer, Cotia, SP, Brasil) foi realizado desgaste superficial da fossa mesial dos primeiros molares superiores e, em seguida, com o auxílio de uma lima K#20, foram realizados pressão apical e movimentos rotacionais até remoção da dentina em uma profundidade de 0,5 mm (identificada pelo travamento do instrumento na cavidade criada) (Figura 3 e Figura 4). Em seguida, foi realizado o capeamento pulpar com o MTA e os dentes foram restaurados com resina flow (Ivoclar, Vaduz, Suíça) fotopolimerizada por 10 segundos (Radii-Call; SDI, Victoria, Austrália) (Figura 5). Os molares do lado oposto não receberam qualquer

intervenção e foram utilizados como controles.

A PBMT foi realizada nos dentes destinados ao grupo MTA/PBMT, antes da aplicação do MTA, e após 24, 48 e 72 horas. Para tanto, foi utilizado laser de diodo de InGaAl (Photon Lase II personalizado; DMC Equipamentos, São Carlos, SP, Brasil), em modo de operação contínuo e aplicação pontual e em contato com o molar. Os parâmetros de dosimetria foram os mesmos utilizados em estudo anterior do grupo de pesquisa (DINIZ *et al.*, 2018; GOMES *et al.*, 2022): 660 nm, 20 mW, 0,71 W/cm², área do feixe de 0,028 cm², 7 s, 0,14 J de energia total por ponto. Sendo assim, foi utilizada a densidade de energia de 5 J/cm² (DINIZ *et al.*, 2018; GOMES *et al.*, 2022; MOREIRA *et al.*, 2017).

Após 7 e 21 dias da primeira aplicação de fotobiomodulação, os animais foram eutanasiados (300 mg/Kg de Cetamina e 30 mg/Kg de Xilazina, via intraperitoneal). Não houve restrição alimentar em qualquer período. Os espécimes foram então coletados e fixados em PFA à 4%, por 24 horas. Após a fixação foram lavados com PBS edesmineralizados por 28 dias em solução de EDTA a 10%, pH 7,4 e em temperatura ambiente.

Figura 1 – Mesa cirúrgica personalizada confeccionada através da impressão 3D.



Fonte: Arquivo pessoal, 2022.

Figura 2 – Primeiro passo na realização da injúria pulpar; aspecto extraoral.



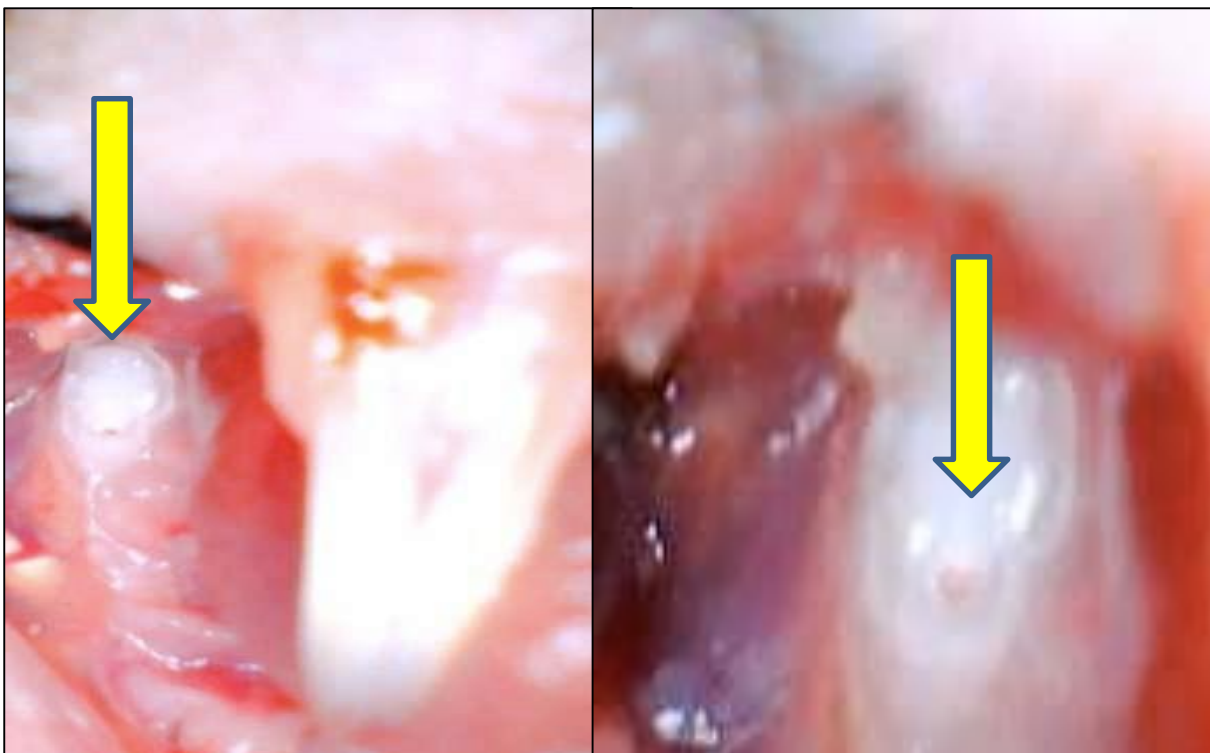
Fonte: Arquivo pessoal, 2022.

Figura 3 – Desgaste superficial com broca LN, seguido pela remoção da dentina com lima endodôntica até o teto da cavidade pulpar.



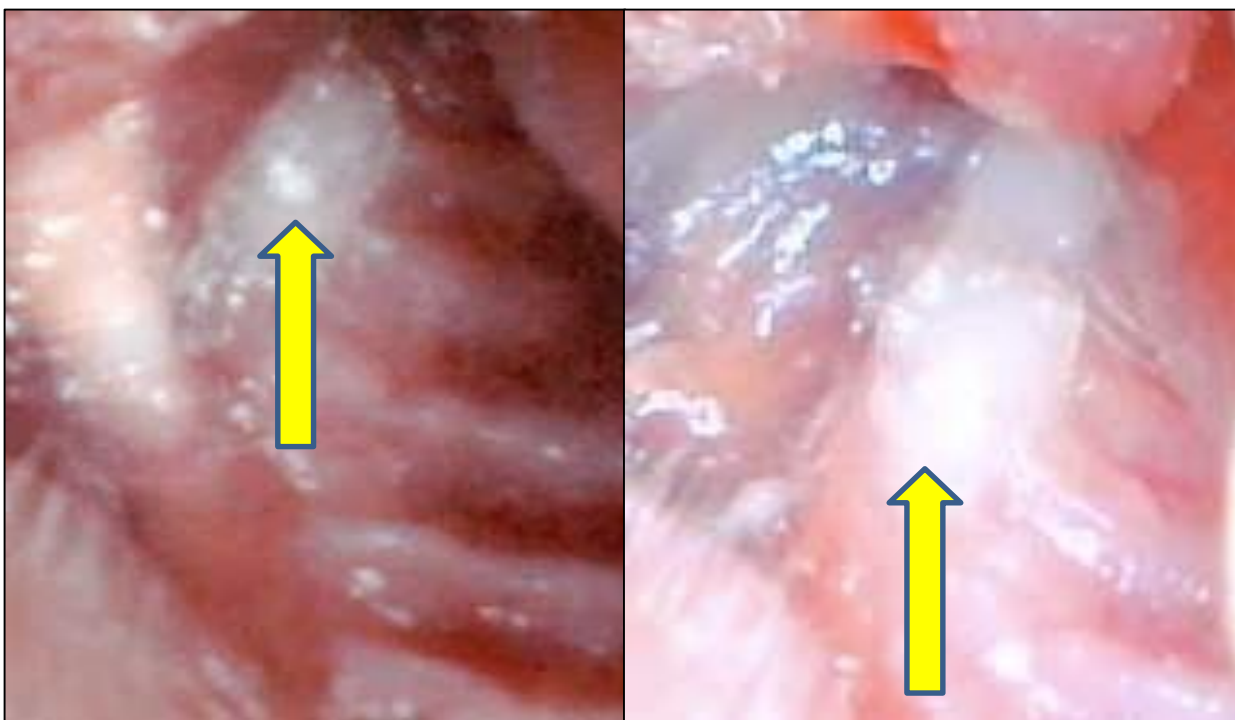
Fonte: Arquivo pessoal, 2023.

Figura 4 – Aspecto final da exposição pulpar, seguida de magnificação com câmera intraoral.



Fonte: Arquivo pessoal, 2023.

Figura 5 – Aspecto final do capeamento pulpar com MTA, seguida de restauração com resina fluida.



Fonte: Arquivo pessoal, 2023.

3.3.2.2 Análises em RT-qPCR

Três amostras de cada grupo foram utilizadas para análise da expressão gênica. Os genes NG2, Nestina, GFAP, CD105 e aqueles relacionados à diferenciação odontogênica (DSPP e RUNX-2) foram analisados por RT-qPCR. Resumidamente, o RNA total foi extraído em tampão de extração pelo método de colunas (RNAeasy, Qiagen, Valencia, CA). Contaminações com DNA genômico foram removidas por tratamento com DNase I. Em seguida, cDNA de cada grupo experimental foi sintetizado utilizando VILO IV (Invitrogen, Carlsbad, CA), seguindo-se as recomendações do fabricante. Em seguida, a análise dos níveis de expressão gênica nos grupos experimentais foi avaliada por reações de qPCR, utilizando-se SYBR Green Dye I e primers relacionados aos genes de interesse. A avaliação da expressão gênica relativa foi feita pelo método $2^{-\Delta\Delta C_t}$, utilizando-se GAPDH (gliceraldeído-3-fosfato desidrogenase) como controle endógeno e os controles hígidos como referência.

Tabela 1. Sequência de primers utilizados para análise qPCR

Gene	Primers
NG2	Forward: 5' - CTGTTCTCACACAGAGGAGCC - 3' Reverse: 5' - TGGACAGACGGTCAACTTCC - 3'
Nestin	Forward: 5' - TGGCTACATACAGGACTCTGC - 3' Reverse: 5' - AAGGATGTTGGGCTGAGGAC - 3'
GFAP	Forward 5'-CTTCCCGCAACGCAGAG-3' Reverse 5'-GAGCCGTGGGCACTAAA-3'
CD105	Forward 5'- TGC ACTTGGCCTACAATTCCA-3' Reverse 5'- AGCTGCCCACTCAAGGATCT-3'
Dspp	Forward: 5' - CTGGGCCATTCCGGTTCC - 3' Reverse: 5' - ATCTCACTGCCATCTGGGGA - 3'
RUNX-2	Forward: 5' - CAGGCAGGTGCTTCAGAACT - 3' Reverse: 5' - GGGGTGTAGGTAAAGGTGGC - 3'
SDF1- α	Forward: 5' CAGTGACGGTAAACCAGTCAGC - 3' Reverse: 5' - TGGCGATGTGGCTCTCG - 3'
TWIST	Forward: 5' - AGG CCG GAG ACC TAG ATG TCA TT - 3' Reverse: 5' - TTG GTC TCT GCT CTT CTA ATT TCC A
P38	Forward: 5' - TGG ATA TTT GGT CCG TGG GC- 3'

	Reverse: 5' - TGC TGA AGC TGG TTA ATA TGG TCT - 3'
GAPDH	Forward: 5' - ACGGCCGCATCTTCTTGTGCA - 3'
	Reverse: 5' - CGCCAAATCCGTTACACCGA - 3'

Fonte: Arquivo pessoal, 2024.

3.3.2.3 Análises Histológicas

3.3.2.4 Microscopia confocal

Os espécimes depois de fixados e desmineralizados como descrito anteriormente na seção de ensaios *in vivo*, foram crioprotetidos com Sacarose 30% overnight e embidos em meio de inclusão Optimum Cutting Temperature OCT. Seções de 25 µm de espessura foram cortadas em criostato e montadas em lâminas de vidro. Os cortes foram contra-corados com DAPI em meio de montagem (Abcam, Cambridge, EUA). Foram utilizadas as objetivas Plan Apo 20x e 40x. As células indiferenciadas marcadas pela fluorescência endógena visualizada em verde (GFP), a população total de pericitos também por marcação endógena vermelha (DsRed) e as subpopulações de pericitos Tipo 1 (colocalização de marcadores DsRed e DAPI em rosa) e Tipo 2 (colocalização de GFP, DsRed e DAPI em amarelo) foram calculadas pela intensidade de fluorescência (valores médios de cinza), após ajuste manual de threshold para todas as amostras, usando o Photoshop (Adobe, San Jose, EUA) e o software Fiji (NIH, Bethesda, EUA).

3.3.2.5 Histologia (H&E e Tricômio de Masson)

Para as análises histoquímicas utilizando a coloração de H&E e Tricômio de Masson, as amostras previamente fixadas e desmineralizadas foram desidratadas em série crescente de álcool, diafinizadas em xilol e incluídas em parafina. Foram então utilizadas seções de 5 µm de espessura dos blocos cortados sagitalmente no sentido vestibulo-lingual em micrótomo (Leica, Wetzlar, Alemanha), os quais foram posteriormente corados com H&E e Tricômico de Masson (TM).

A arquitetura tecidual e a graduação do processo inflamatório, observada nas lâminas coradas com H&E, foram analisados de acordo com Løvschall *et al.*, 2007. Para

tanto, dez campos histológicos dos cornos distais, médios e mesiais (região injuriada) de cada grupo experimental foram selecionados aleatoriamente e analisados (400x) da seguinte maneira: (1) Vitalidade pulpar: vitalidade total da polpa dentária coronária (++) , vitalidade parcial da polpa dentária coronária (+) e não vital (-). Polpa com tecido necrótico ou ausência de tecido dentro da câmara pulpar foram consideradas não vitais, enquanto amostras com tecido pulpar representadas por tecido conjuntivo vascularizado foram vitais; (2) Sinais inflamatórios: apenas as amostras classificadas como vitais (++ e +) foram avaliadas para a condição do tecido pulpar distante da injúria, designadas como: presença de apenas um dos sinais inflamatórios (+), dois sinais de inflamação (++) , mais de dois sinais inflamatórios (+++), ou ausência de inflamação (-). Os sinais inflamatórios considerados foram: vasos sanguíneos dilatados e congestionados; glóbulos vermelhos fora dos vasos; infiltração de células inflamatórias (como leucócitos polimorfonucleares e neutrófilos); e microabscessos.

Para observar a formação de barreira dentinária e mineralização na polpa dentária utilizamos a coloração de Tricômio de Masson, seguindo as recomendações do fabricante. Para cada seção histológica, três campos consecutivos da coroa com aumento de 20 e 40x foram selecionados para a análise. Analisamos a presença de dentina terciária, ponte dentinária e calcificações na polpa dentária (ABRAHÃO *et al.*, 2006). Todas as amostras foram observadas em um microscópio óptico (DM 4000 B, Leica®, Germany) e todas as análises histológicas foram realizadas por um examinador calibrado e cego

3.3.2.6 Análise Estatística

Os dados foram tabulados e submetidos aos testes de normalidade. Testes estatísticos posteriores foram aplicados considerando um nível de confiança de 95% para avaliar as diferenças entre os grupos. Foram aplicados o teste t não-pareado ou ANOVA seguido de Tukey, em caso de dados paramétricos, e o teste de Mann-Whitney ou Kruskal-Wallis seguido de Dunn, em casos de dados não paramétricos.

4 RESULTADOS

4.1 Articulo 1

Mapping pericytes and neural progenitors' temporo-spatial distribution during postnatal odontogenesis and dental aging in Nestin⁺NG2⁺transgenic mice

Abstract

The ectomesenchymal components of dental pulp exhibit different levels of plasticity and self-renewal potential. Understanding how dental pulp stem cells (DPSCs) influence dental formation and aging could guide future endodontic therapeutic strategies and prognosis. DPSCs play a role in tooth morphogenesis and part of them remain in the dental pulp as a reserve of cells involved in its repair following injury. In this context, we examined markers for neural progenitors (Nestin/GFP) and pericytes (NG2/DsRed) at different stages of mice model (C57BL/6) life: one day, 14 days, 2 months, and 12 months old. NG2⁺ pericytes appear to function as progenitor cells for odontoblasts during odontogenesis, serving as key components in the formation of primary, secondary, and possibly, tertiary dentin in response to low-intensity stimuli in adult teeth. We hypothesize that NG2⁺ cells dispersed in the central region of the dental pulp, or those that remain closely associated with the microvasculature of the dental pulp, may have additional functional roles, including phagocytic and immunological functions, and may also be recruited in response to specific conditions. Furthermore, it is suggested that Nestin-expressing neural progenitor cells are a less compromised source of dental pulp stem cells capable of differentiating into odontoblasts through NG2 expression, particularly when dentinogenesis is required. Here we demonstrate that NG2 can be expressed in the odontoblast layer during early stages of dentinogenesis and also in regions compatible with contracted stimuli where odontoblast activity is required. Nestin was present not only in the formation of the dental papilla but also in the stellate reticulum that would give rise to two distinct tissue types, dentin and enamel respectively.

Introduction

During odontogenesis, a series of orchestrated cellular and molecular events culminate in tooth formation (Cobourne, 1999). The anatomy, positioning, and size of teeth depend on the proliferation, differentiation, and apoptosis of different cell populations. This process is governed by a complex temporo-spatial interaction between the oral epithelium, derived from the ectoderm, and the ectomesenchyme, which is invaded by neural crest cells, and is regulated by the expression of various genes (Bei, 2009, Berkovitz *et al.*, 2004, Bluteau *et al.*, 2008, Katchburian, Arana 2004).

Nestin is a ubiquitous component of the cytoskeleton and an embryonic marker for neural stem cells involved in dental development and dentin repair processes. However, it has been demonstrated that nestin expression can be upregulated by adjunctive therapies in response to dental pulp injury (Gomes *et al.*, 2022). Additionally, it has been positively regulated by odontogenic epithelium stimulation in odontogenic mixed tumors (Fujita *et al.*, 2006). Pericytes, on the other hand, are perivascular cells with stem cell characteristics that may co-express nestin (Birbrair, 2013, Birbrair, 2014, Gomes *et al.*, 2020). Pericytes are known for their ability to differentiate into odontoblasts *in vivo* (Shi, Gronthos 2003) and participate in the process of repair of injured dental pulp (Feng *et al.*, 2011, Gomes *et al.*, 2022). Recently, we demonstrated the existence of two subpopulations of pericytes within the dental pulp: the Nestin-NG2⁺ and Nestin⁺NG2⁺ subsets (Gomes *et al.*, 2022). However, the functional role of each subset has yet to be established.

Considering that neural progenitors and pericytes have demonstrated the ability to differentiate into odontoblasts and have been observed in dental pulp repair processes, understanding the role of these cells in odontogenesis and tooth aging can make them promising targets for regenerative procedures, such as cell-homing therapies. In this study, we employed a transgenic mice model (C57BL/6) expressing specific fluorescent reporters for Nestin and NG2 proteins, allowing us to map the distribution of neural progenitors and pericytes during postnatal odontogenesis at 1 and 14 days, 2-month-old adults, and 12-month-old aged teeth.

Methods

Animal Model

The study was approved by the Animal Care and Use Committee of the Federal University of Minas Gerais (protocol No. 181/2020). The expected Nestin GFP/NG2 DsRed phenotypes were obtained as previously described (Birbrair *et al.*, 2013). All animals were housed under temperature-controlled environment (22°C–24°C) and under a 12:12 hour light-dark cycle and *ad libitum* access to feed and water.

Male or female Nestin GFP/NG2 DsRed mice, aged 1 day, 14 days, 2 months and 12 months (n = 3/group) were used in this study. The animals were phenotyped to determine if they expressed a positive phenotype for Nestin and NG2. The positive animals were euthanized with anesthetic overdose (100mg/Kg Ketamine + 10mg/Kg Xylazine, administered intraperitoneally), and their maxillae and mandibles were collected. The specimens were fixed in 4% paraformaldehyde overnight at room temperature, then demineralized in 10% EDTA. The 2- and 12-month groups were demineralized for 21 days, while the 1-day and 14-day groups were demineralized for 3 days. Afterward, they underwent cryoprotection in 30% sucrose for 24 hours. The samples were reduced, retaining only the hemimaxilla area for sectioning, then embedded in Tissue-Tek® O.C.T. Compound (Sakura Finetek USA, Torrance, California) and sectioned at a thickness of 25 µm using a cryostat (Leica Biosystems, Nussloch, Germany). Finally, the sections were post-fixed in methanol, mounted with mounting medium, counterstained with DAPI (Thermo Fisher Scientific, Waltham, Massachusetts), and prepared for imaging via confocal microscopy.

Confocal analysis

Cells were examined using an Eclipse Ti microscope equipped with a confocal head, model LSM 880 (Zeiss, Oberkochen, Germany). The objectives used were Plan Apo 20x and 40x. For each sample, a large sweep image was captured using the 10x objective. Analysis was performed in the sagittal plane, from buccal to lingual, with the point of interest defined by the visualization of the three pulp horns and the complete roots of adult teeth (at 2- and 12-month experimental time points) or the developing dental germs and complete dental follicles. Channels were analyzed both separately and together to observe co-localizations. NG2+ cells were visualized via red fluorescence, Nestin-expressing cells were observed through green fluorescence, and

co-localization of the markers appeared in yellow. The fluorescence threshold was manually adjusted, and the fluorescent area was analyzed using Fiji software (NIH) by a trained researcher.

Results

At one postnatal day, teeth in the bell phase exhibited intense Nestin-positive cells in the oral epithelium and the stratum intermedium. Nestin+ cells were also detected within the stellate reticulum, with a concentration near the stratum intermedium. In the dental papillae, a few scattered Nestin+ cells were observed, primarily distributed around the periphery and at the horns of this tissue. Some structures suggestive of blood vessels in the dental follicle region, at the base of the dental papillae, also exhibited Nestin+ cells co-localized with NG2+ cells. Subpopulations of Nestin+NG2+ were detected as part of a supposed blood vessel endothelium, as well as dispersed in the dental papillae. NG2+ cells were mostly present in the dental follicle region, particularly in the alveolar bone primitive structure (Figure 1).

At the first sign of reciprocal induction between preameloblasts and preodontoblasts, the deposition of the dentin mantle and the polarity inversion of ameloblasts were observed. Accordingly, in the late bell stage, upregulation of Nestin and NG2 was compartmentalized within the dental papilla, particularly in the horns with more advanced stage of development. Preodontoblast cells appear strongly stained with NG2, while an adjacent layer of Nestin+ cells was organized in the region corresponding to the cell-rich zone (Figure 2).

The fusion of the reduced enamel epithelium with the oral mucosa indicated that the tooth was about to emerge into the oral cavity in the 14-day-old normal mice (Figure 3 and 4). The reduced enamel epithelium of a tooth in its eruptive phase is also showed upregulation of Nestin protein (Figure 3 and 4). Furthermore, well-defined dentin and enamel tissues are observed in the crown phase (14-day-old mice). At that time point, the expression of NG2 decreased abruptly and was almost absent in the region corresponding to the odontoblasts. Instead, NG2+ cells are observed in the central region of the dental papilla, frequently associated with structures suggestive of blood vessels, and sometimes co-localized with Nestin+ cells. NG2+ cells continued to be the predominant marked components within the alveolar bone surrounding the dental

follicle.

The teeth of the animal group at two months of age presented an odontoblast layer with cells showing dimmer Nestin+ fluorescence compared to the cell-rich zone, which holds the great majority of Nestin-expressing neural progenitors. Nestin+NG2+ were rare, dispersed within the cell-rich zone at the periphery of the pulp chamber and along roots. NG2+ cells are located mostly in perivascular niches in the central part of the pulp tissue but also eventually appear within the odontoblast layer. Qualitatively, more NG2+ cells were observed in adult teeth compared to the 1 and 14-day-old teeth. Cementoblasts in the roots and osteoblasts in the alveolar bone also markedly express the NG2 protein. A few Nestin+ or Nestin+NG2+ cells dispersed in the periodontal ligament and gingival papillae completed the Nestin-GFP and NG2-DsRed fully developed tooth reporter scenario (Figure 5).

A twelve-month-old tooth submitted to physiological stimuli typical of rodent animals is depicted in Figure 6. Signs of dental pulp atresia due to dentin deposition were regularly present. Nestin expression appeared dimmer and more discontinuous in the cell-rich zone layers of aged teeth compared to the younger ones. At the very top of dental pulp horns, Nestin expression was almost totally absent. Interestingly, a reexpression of NG2 in the odontoblast layer was observed in the horn areas corresponding to the external stimulus of enamel wear. NG2+ cells remained dispersed in the central region of the dental pulp, particularly close to the microvasculature. Similarly to adult teeth, cementoblasts and the alveolar bone remarkably expressed the NG2 protein (Figure 6)

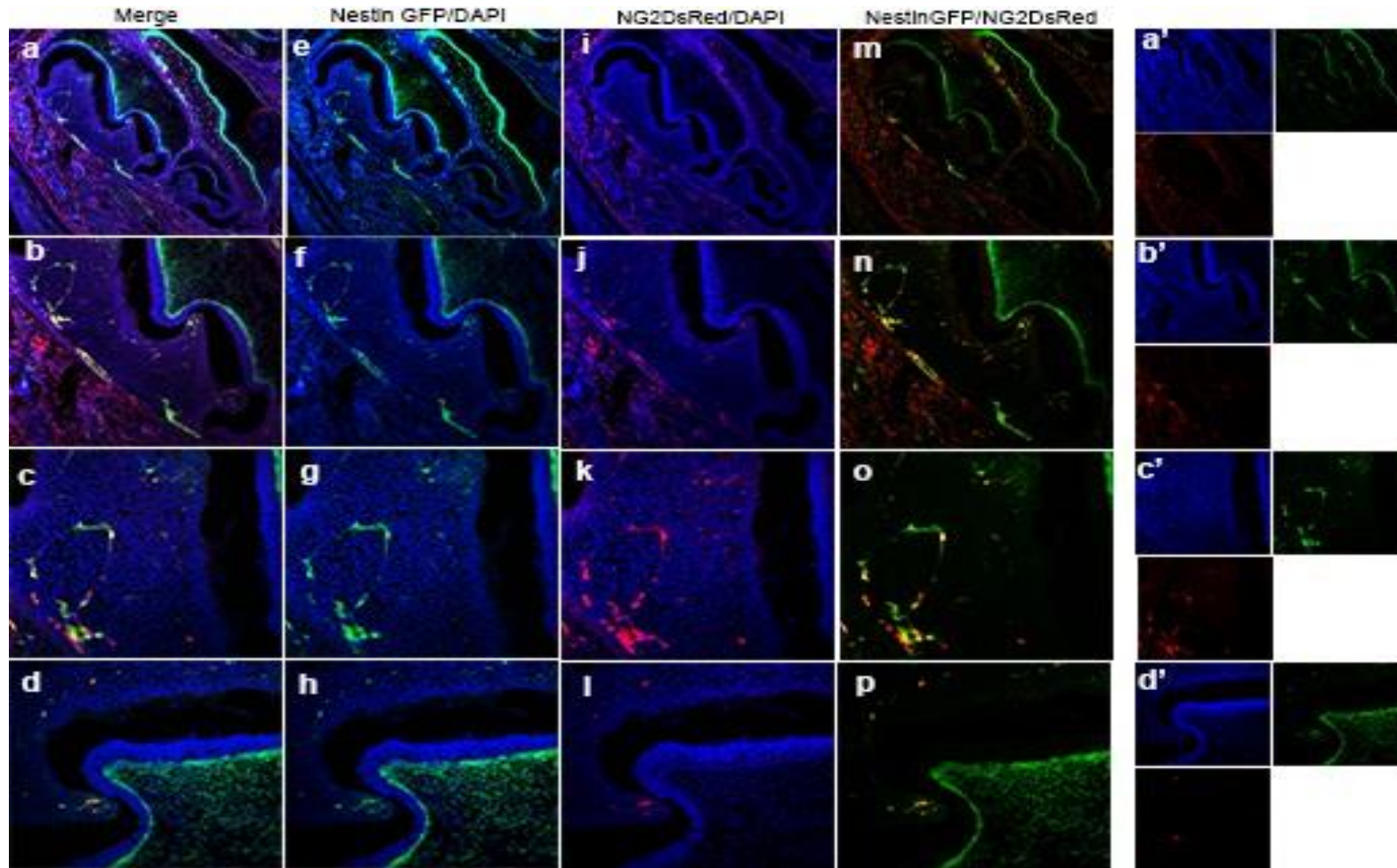


Figure 1 - Labelled Cells Characterization in Postnatal Odontogenesis. Representative image of Nestin⁺ and NG2⁺ cells observed under confocal microscopy during 1-day-old neonatal odontogenesis. In (a, b, c, d), we can see the merge of fluorescence channels for Dapi, Nestin, and NG2 demonstrating the developing tooth germ at 10x magnification (a), the dental papilla and dental follicle structures at 20x magnification (b), the dental papilla with details at 40x magnification (c), the stellate reticulum and intermediate stratum at 40x magnification (d). In images (e, f, g, h), we have the Nestin and Dapi channels selected, showing that Nestin⁺ cells are concentrated in the stellate reticulum region (h), central regions of the dental papilla (g), and at the periphery of the dental follicle (f). In (i, j, k, l), we observe the NG2 and Dapi channels together, noting the pericytes distributed in the dental papilla (k) and dental follicle (j), absent in the other regions analyzed here. In (m, n, o, p), we merge the NG2 and Nestin channels and observe their co-localization in cells of the dental papilla and follicle in regions suggestive of blood vessels. Images a', b', c', d' represent individual fluorescence channels.

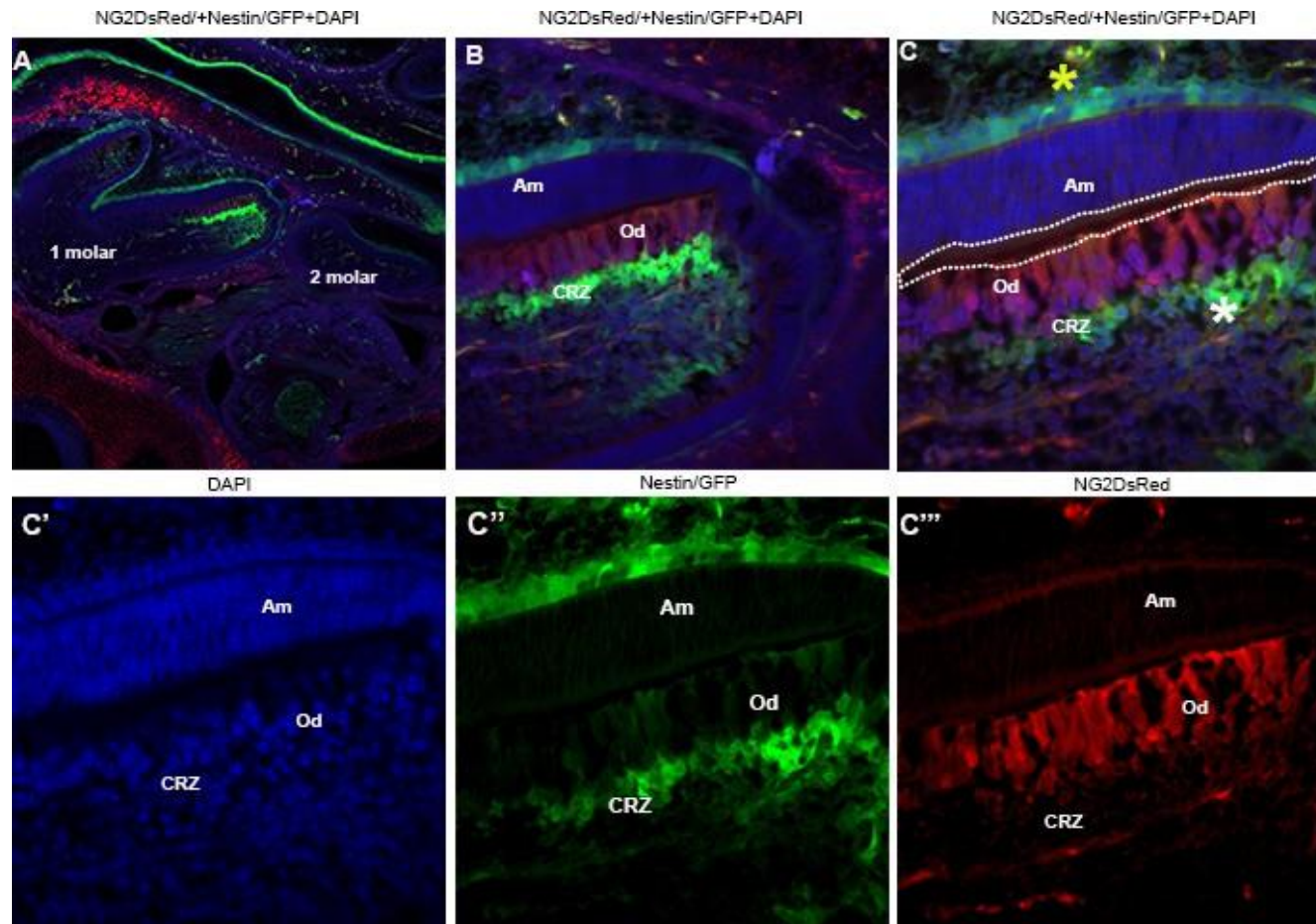


Figure 2 - Characterization of cells after mantle dentin production in odontogenesis. In (A), we have the fluorescent image of all selected channels demonstrating the formation of the first and second molars, and it is possible to observe a different cell pattern between the two elements (10x). In (B), we have an enlarged image with all selected channels focusing on the formation of what would be the cusp of this element, showing a cell compartmentalization pattern (20X). We have an image focusing on the layer of pre-ameloblasts (Am) and young odontoblasts (Od) in (b-c). Note the conformation of NG2-positive cells in the odontoblast layer with characteristics of nuclear polarization, the cell-rich zone populated by Nestin-positive cells (CRZ), and the palisading pre-ameloblasts. In (B-C), we highlight a dotted line image suggestive of the deposition of acellular tissue consistent with mantle dentin. In (c', c'', c'''), we have the separate channels confirming the compartmentalized organization of these cells.

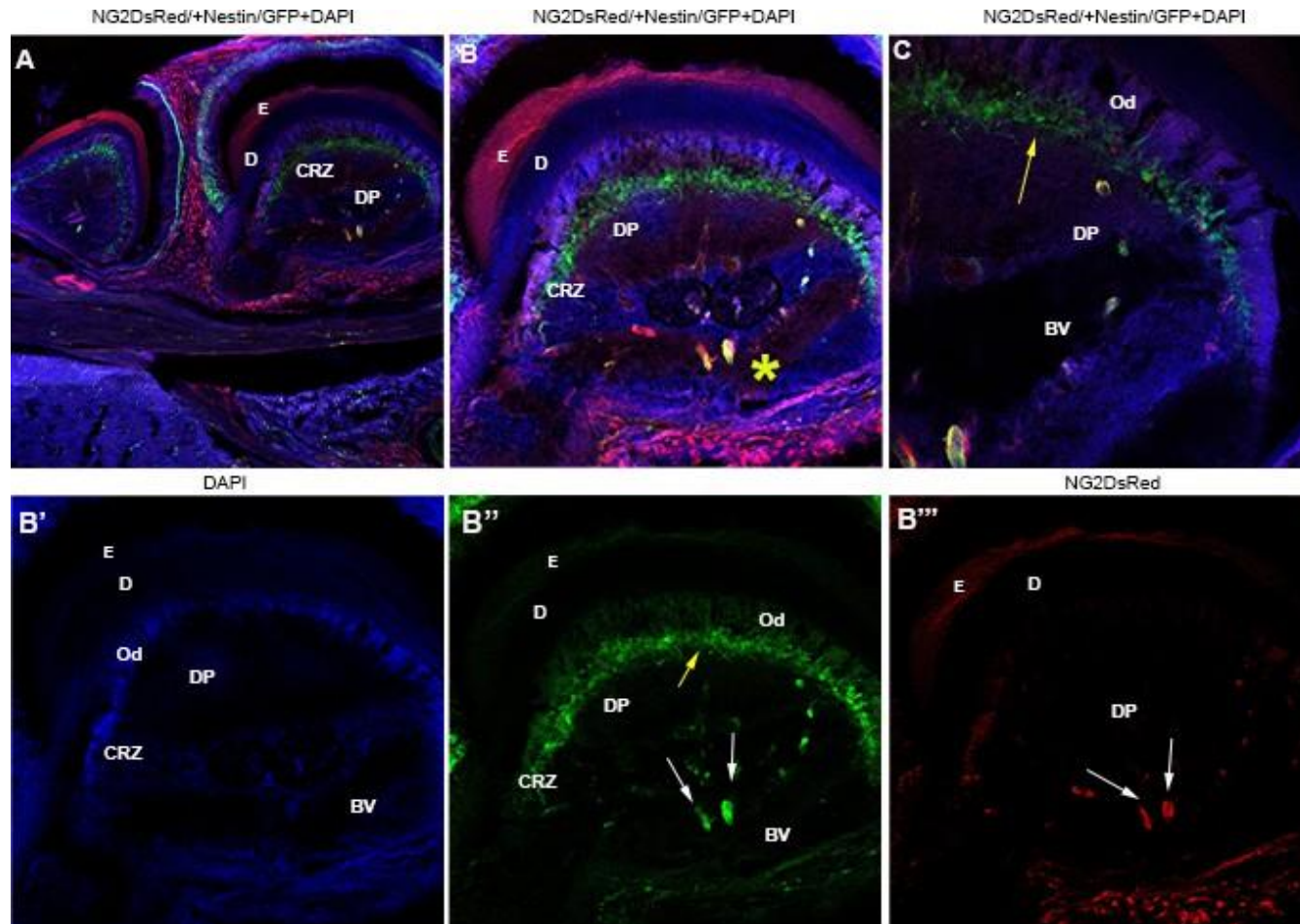


Figure 3 - Characterization of cells after mantle dentin production in odontogenesis. Sagittal sections of 14-day-old transgenic neonatal mouse teeth are depicted in the images above. In sections A, B, and C, merged fluorescence channels show the arrangement of Nestin and NG2 cells in this formation phase (B-C). We observe the co-localization of these cells highlighted by * (B) white arrows (B'' - B'''). Nestin is observed in the cell-rich zone (CRZ) layer just below the newly formed odontoblast layer, indicated by the yellow arrow (C and B''). E = Enamel, D = Dentin, Od = Odontoblasts, DP = Dental Papilla, BV = Blood Vessels, CRZ = Cell-Rich Zone.

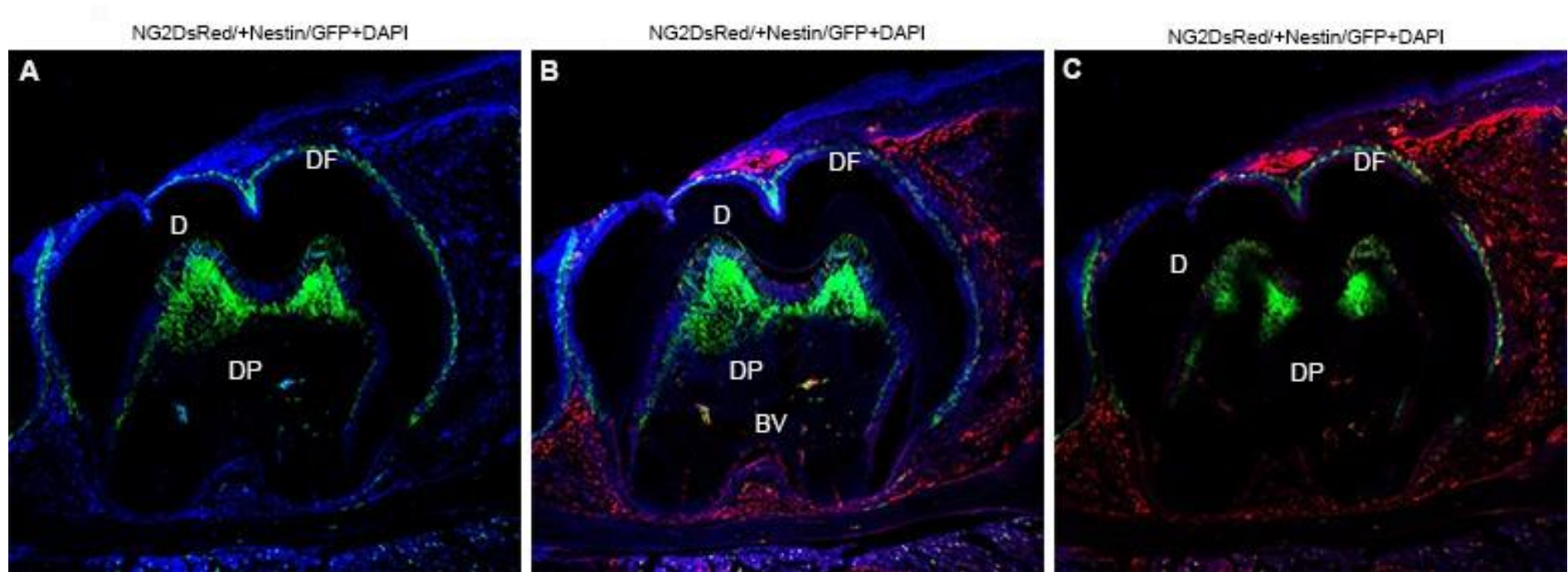


Figure 4 - Demonstration of the same tooth at different cutting depths. We observe a tooth in an eruptive phase. Note the presence of Nestin cells represented by green fluorescence surrounding the dental follicle (DF), and concentrated in the pulp horn where the coronal pulp already presents a well-defined morphology and formed dentin (D). Large blood vessels can also be observed (BV). NG2 cells are dispersed in the region of the dental pulp (DP) and alveolar bone.

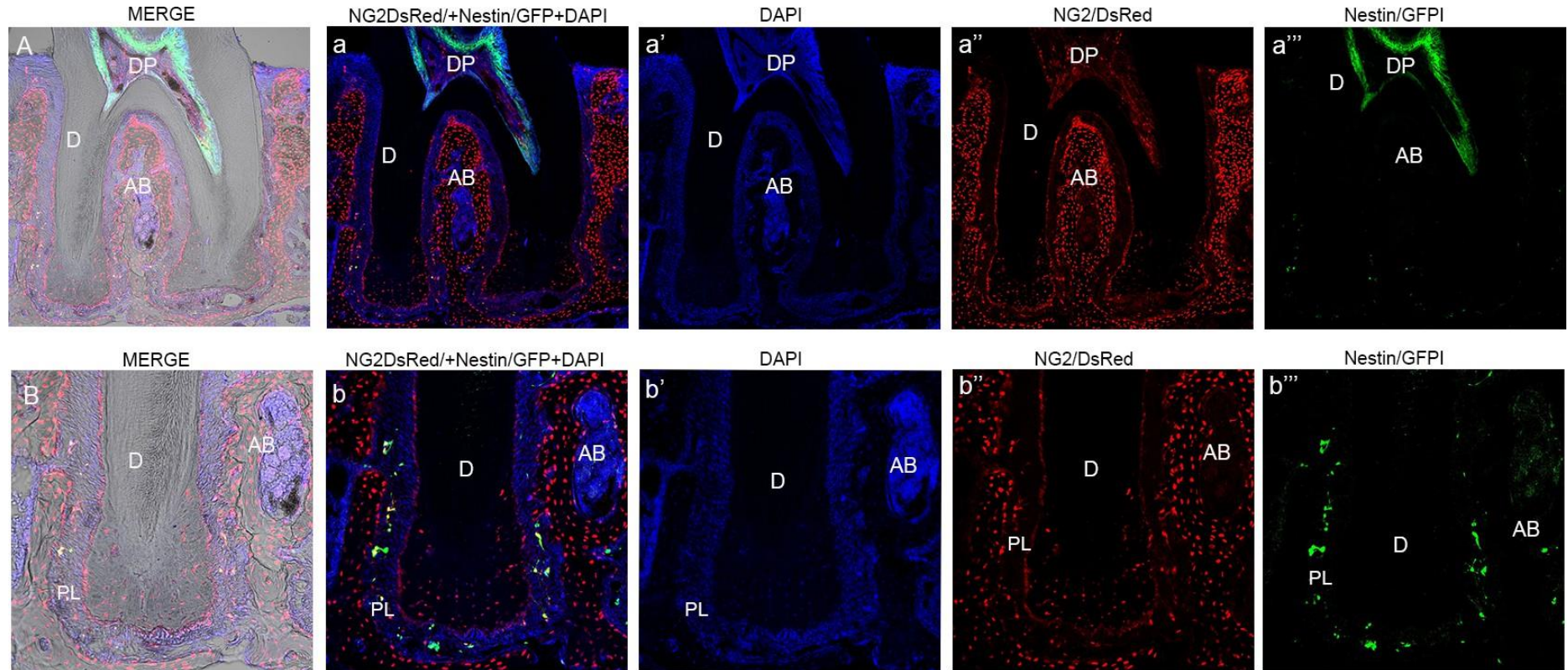


Figure 5 - Characterization of Nestin and NG2 cells in young adult teeth. We demonstrate the compartmentalized organization of neural origin stem cells and pericytes in dental pulp and surrounding tissues. (A, a, B, b) We have Nestin + fluorescence cells in the discrete odontoblastic layer that becomes evident in the cell-rich zone. (a'') We observe Nestin+ cells in the region of the root apex, more specifically in the periodontal ligament (b'''), sometimes presenting co-localization with NG2+ cells (b-b''). NG2+ cells are located in perivascular niches in the central region of the pulp tissue (a-a''). Cementoblasts in the roots and osteoblasts in the alveolar bone also markedly express the NG2 protein (b-b'').

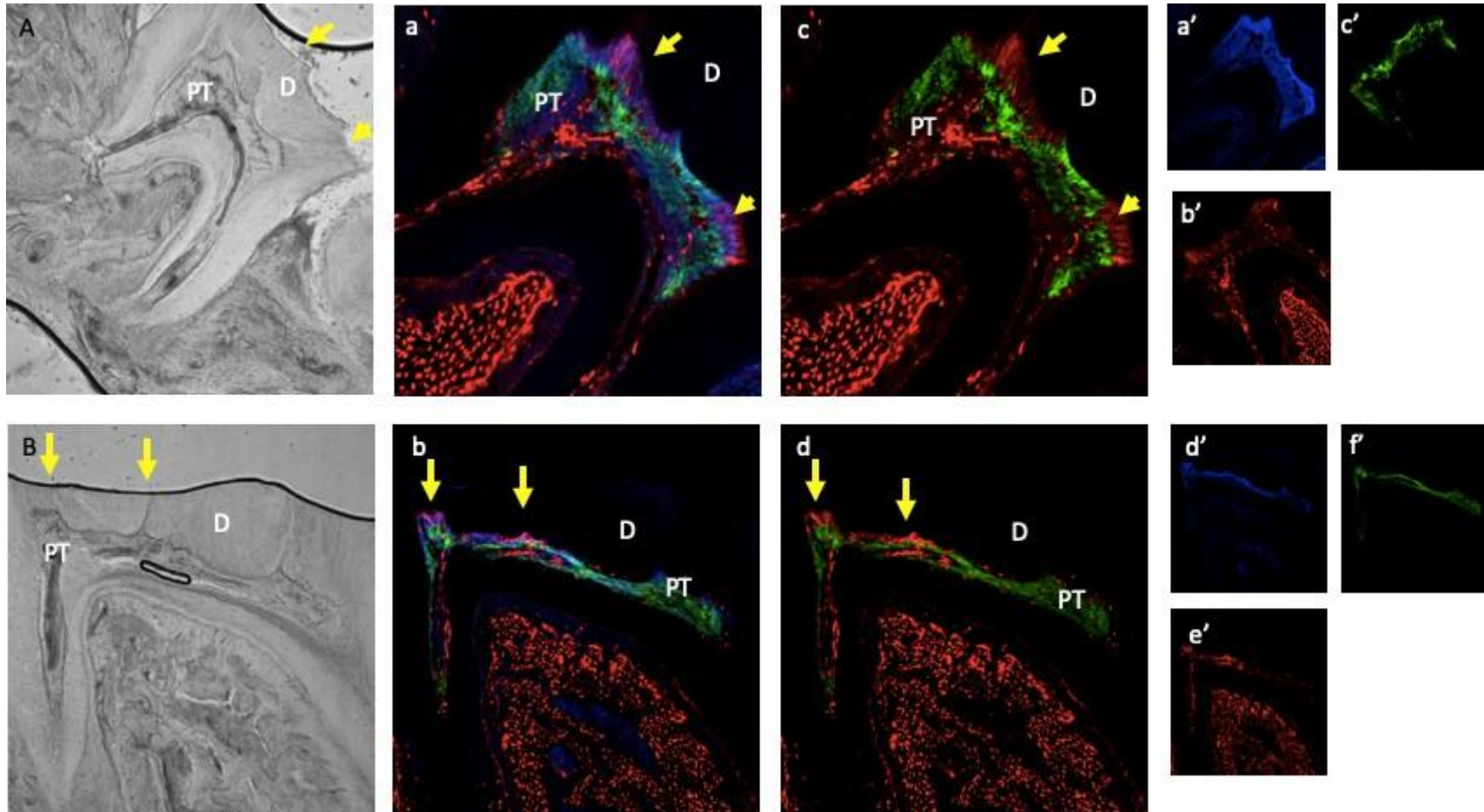


Figure 6 – Characterization of cells after natural occlusal wear in mature teeth. Labeled cell localization in aged teeth and after exposure to natural wear stimuli. (A - B) Representative sagittal bright-field sections of two molars from different animals (a - b) Merge of Dapi, Nestin, and NG2 channels at 20x. Note that pericytes appear increased in the area corresponding to the external wear highlighted by the arrows. (c - d) Merged Nestin-GFP and NG2 channels. Note that some pericytes are located in the central region of the pulp tissue, while others are concentrated in the odontoblast region, but neural cells remain localized in the region of the cell-rich zone of the dental pulp (CRZ). In (a', b', c', d', e', f'), we have the separate channels.

Discussion

Interactions between oral epithelial cells and the underneath mesenchyme occur to initiate odontogenesis. Sequential and reciprocal cellular events of morphology and cytodifferentiation are part of this process (Thesleff and Hurmerinta, 1981, Lumsden, 1988). In this study, we investigated the Nestin and NG2 markers, as they may represent relevant stem cell populations. Nestin is a marker of neural stem cells previously studied in neural and muscular tissues, and is expressed in early stages of development (Sjoberg *et al.*, 1990). During odontogenesis, Nestin exhibits different expression patterns within dental tissues. Initially, regions that will give rise to dental enamel, such as the stellate reticulum and intermediate stratum, show considerable quantities of Nestin+ cells, which decrease as tooth formation progresses. In regions that will give rise to dental pulp, such as the dental papilla, this expression gradually increases from the beginning to the end of tooth formation (Terling *et al.*, 1995, Liu *et al.*, 2019). In our model, we confirmed this hypothesis, where Nestin+ cells appeared in the stellate reticulum and the central region of the dental papilla at the onset of odontogenesis, distributed in this manner, and then decreased after ameloblast differentiation but increased in dental pulp until dental aging.

Nestin can also be considered a marker for young odontoblasts (Mitsiadis 2001). It is speculated to have an inductive role and maintain the cytoskeleton of dental tissue, being expressed in ameloblasts and odontoblasts during the cytodifferentiation phase (Terling *et al.*, 1995). We have demonstrated that in stages where mantle dentin is secreted, cells in the odontoblastic layer begin to express NG2 and appear to be supported by an adjacent layer of Nestin+ cells, suggesting that this cytodifferentiation may involve pericytes induced or not by Nestin+ cells. Further studies could confirm this relationship.

Furthermore, authors have suggested that Nestin is absent in permanent teeth and may be selectively expressed in teeth in response to pathological stimuli (Mitsiadis 2001). However, our model has demonstrated that Nestin is indeed present in adult teeth, and it appears that the differentiation of odontoblasts in response to harmful stimuli is primarily influenced by pericytes, aligning with more studies (Lovschall *et al.*, 2007, Feng *et al.*, 2011, Gomes *et al.*, 2022). Nonetheless, this does not rule out the possibility of neural cells playing a role in the induction or recruitment of pericytes to

the injured area; we cannot make a definitive statement on this matter at this time.

Perivascular stem cells possess the capability for odontogenic differentiation, and pericytes represent a subset of these cells that can differentiate into odontoblasts, participating in the forefront of pulp repair. NG2 serves as a marker for pericytes and perivascular mesenchymal stem cells (Bakopoulou *et al.*, 2013, Lovschall *et al.*, 2007, Feng *et al.*, 2011, Kaukua *et al.*, 2014, Gomes *et al.*, 2022). In our model, we have observed pericytes exhibiting morphology identical to that of newly undifferentiated odontoblasts, secreting mantle dentin during odontogenesis and reparative dentin in aged teeth within the odontoblastic layer.

A portion of the stem cells within dental pulp may have both neural and perivascular origins (Shi and Gronthos, 2003). In our study, we have noted the co-localization of Nestin and NG2 markers, primarily during the early stages of dental formation.

When tracing a chronological sequence, we initially observe that during the proliferation and morphodifferentiation phase, there is a limited presence of Nestin and NG2 cells co-localized in regions of the dental papilla near structures resembling blood vessels. Subsequently, in the cytodifferentiation phase, we observe a segregation of these cells, with the expression of NG2 occurring in the layer of newly differentiated odontoblasts, which are already secreting mantle dentin. This layer of odontoblasts is supported by a layer of Nestin-positive cells. These findings contradict studies suggesting that pericytes can differentiate into odontoblasts, while Nestin-positive cells demonstrate inductive capabilities in cytoskeletal maintenance (Bakopoulou *et al.*, 2013, Lovschall *et al.*, 2007, Feng *et al.*, 2011, Kaukua *et al.*, 2014, Gomes *et al.*, 2022, Terling *et al.*, 1995).

During the dentin and enamel apposition phases, pericytes appear to decrease their presence within the odontoblastic layer and re-emerge in the central region of the pulp in close proximity to the developing microvasculature, likely fulfilling their role in vascular formation and stabilization, as well as blood flow regulation (Birbrair *et al.*, 2013, Pallone *et al.*, 2003). Conversely, Nestin-positive cells maintain their positioning, reinforcing the notion that they are responsible for cytoskeletal maintenance under healthy conditions (Couve *et al.*, 2018).

In fully formed teeth, we have observed the preserved layer of Nestin-positive cells, while pericytes were observed in regions affected by physiological dentin wear. This observation aligns with current studies suggesting that pericytes serve as an

additional source of activated cells in response to injury (Feng *et al.*, 2011, Kaukua *et al.*, 2014, Løvschall *et al.*, 2007, Vidovic *et al.*, 2017, Vidovic-Zdrilic *et al.*, 2018, Gomes *et al.*, 2022). To determine whether these cells were indeed recruited from the bloodstream, an experimental reporter model could provide valuable insights.

This study mapped stem cells at different stages throughout the formation and functional lifespan of a tooth, using a transgenic murine model (NG2 DsRed/Nestin GFP) to trace pericytes (NG2) and undifferentiated cells (Nestin). Our key findings indicate that pericytes are involved in odontoblast differentiation and dentinogenesis, both in response to noxious stimuli and during early odontogenesis, with NG2 being a potential marker for newly differentiated odontoblasts. Additionally, this study demonstrated that neural progenitors (Nestin+ cells) appear to orchestrate odontoblast differentiation, playing a crucial role in cytoskeletal maintenance. These cells can be expressed in mesenchymal and epithelial lineages, such as the stellate reticulum. Further studies with genetic tracking are needed to confirm the temporality of these cellular markers and strengthen our hypotheses.

REFERENCES

1. Bakopoulou A, Leyhausen G, Volk J, Koidis P, Geurtsen W. Comparative characterization of STRO-1(neg)/CD146(pos) and STRO-1(pos)/CD146(pos) apical papilla stem cells enriched with flow cytometry. *Arch Oral Biol.* 2013 Oct;58(10):1556-68. doi: 10.1016/j.archoralbio.2013.06.018. Epub 2013 Jul 18. PMID: 23871383.
2. Bei M. Molecular genetics of tooth development. *Curr Opin Genet Dev.* 2009 Oct;19(5):504-10. doi: 10.1016/j.gde.2009.09.002. Epub 2009 Oct 28. PMID: 19875280; PMCID: PMC2789315.
3. Berkovitz BKB, Holland GR, Moxham BJ. *Anatomia, embriologia e histologia bucal.* 3^a ed. Porto Alegre: Artmed; 2004. Capítulo 21, Desenvolvimento inicial do dente; p. 290-303.
4. Birbrair A, Zhang T, Wang ZM, Messi ML, Mintz A, Delbono O. (2013). Type-1 pericytes participate in fibrous tissue deposition in aged skeletal muscle. *Am J Physiol Cell Physiol.* 305(11):C1098-113. PMID: 24067916.
5. Birbrair A, Zhang T, Wang ZM, Messi ML, Mintz A, Delbono O. Pericytes: multitasking cells in the regeneration of injured, diseased, and aged skeletal muscle. *Front Aging Neurosci.* 2014 Sep 18;6:245. doi: 10.3389/fnagi.2014.00245. PMID: 25278877; PMCID: PMC4166895.
6. Bluteau G, Luder HU, De Bari C, Mitsiadis TA. Stem cells for tooth engineering. *Eur Cell Mater.* 2008 Jul 31;16:1-9. doi: 10.22203/ecm.v016a01. PMID: 18671204.
7. Cobourne MT. The genetic control of early odontogenesis. *Br J Orthod.* 1999 Mar;26(1):21-8. doi: 10.1093/ortho/26.1.21. PMID: 10333884.
8. Couve E, Lovera M, Suzuki K, Schmachtenberg O. Schwann Cell Phenotype Changes in Aging Human Dental Pulp. *J Dent Res.* 2018 Mar;97(3):347-355. doi: 10.1177/0022034517733967. Epub 2017 Oct 3. PMID: 28972819.
9. Fujita S, Hideshima K, Ikeda T. Nestin expression in odontoblasts and odontogenic ectomesenchymal tissue of odontogenic tumours. *J Clin Pathol.* 2006 Mar;59(3):240-5. doi: 10.1136/jcp.2004.025403. PMID: 16505272; PMCID: PMC1860355.
10. Shi S, Gronthos S. Perivascular niche of postnatal mesenchymal stem cells in human bone marrow and dental pulp. *J Bone Miner Res.* 2003 Apr;18(4):696-704. doi: 10.1359/jbmr.2003.18.4.696. PMID: 12674330.
11. Feng J, Mantesso A, De Bari C, Nishiyama A, Sharpe PT. Dual origin of mesenchymal stem cells contributing to organ growth and repair. *Proc Natl Acad Sci U S A.* 2011 Apr 19;108(16):6503-8. doi: 10.1073/pnas.1015449108. Epub 2011 Apr 4. PMID: 21464310; PMCID: PMC3081015.

12. Gomes NA, do Valle IB, Gleber-Netto FO, Silva TA, Oliveira HMC, de Oliveira RF, Ferreira LAQ, Castilho LS, Reis PHRG, Prazeres PHDM, Menezes GB, de Magalhães CS, Mesquita RA, Marques MM, Birbrair A, Diniz IMA. Nestin and NG2 transgenes reveal two populations of perivascular cells stimulated by photobiomodulation. *J Cell Physiol.* 2022 Apr;237(4):2198-2210. doi: 10.1002/jcp.30680. Epub 2022 Jan 17. PMID: 35040139.
13. Katchburian E, Arana V. *Histologia e embriologia oral.* 2ª ed. Rio de Janeiro: Guanabara Koogan; 2004. Capítulo 6, Odontogênese; p. 147-75.
14. Kaukua N, Shahidi MK, Konstantinidou C, Dyachuk V, Kaucka M, Furlan A, An Z, Wang L, Hultman I, Ahrlund-Richter L, Blom H, Brismar H, Lopes NA, Pachnis V, Suter U, Clevers H, Thesleff I, Sharpe P, Ernfors P, Fried K, Adameyko I. Glial origin of mesenchymal stem cells in a tooth model system. *Nature.* 2014 Sep 25;513(7519):551-4. doi: 10.1038/nature13536. Epub 2014 Jul 27. PMID: 25079316.
15. Løvschall H, Giannobile WV, Somerman MJ, Jin, *et al.* Stem cells and regeneration of injured dental tissue. In: *Textbook and Color Atlas of Traumatic Injuries to the Teeth.* Andreasen JO, Andreasen FM, Anderson L, editors Blackwell Pub Professional, 2007.
16. Liu Q, Du J, Fan J, Li W, Guo W, Feng H, Lin J. Generation and Characterization of Induced Pluripotent Stem Cells from Mononuclear Cells in Schizophrenic Patients. *Cell J.* 2019 Jul;21(2):161-168. doi: 10.22074/cellj.2019.5871. Epub 2019 Feb 20. PMID: 30825289; PMCID: PMC6397609.
17. Lumsden AG. Spatial organization of the epithelium and the role of neural crest cells in the initiation of the mammalian tooth germ. *Development.* 1988;103 Suppl:155-69. doi: 10.1242/dev.103.Supplement.155. PMID: 3250849.
18. Mitsiadis TA. Molecular aspects of tooth pathogenesis and repair: in vivo and in vitro models. *Adv Dent Res.* 2001 Aug;15:59-62. doi: 10.1177/08959374010150011501. PMID: 12640742.
19. Sjöberg G, Edström L, Lendahl U, Sejersen T. Myofibers from Duchenne/Becker muscular dystrophy and myositis express the intermediate filament nestin. *J Neuropathol Exp Neurol.* 1994 Jul;53(4):416-23. doi: 10.1097/00005072-199407000-00014. PMID: 8021716.
20. Terling C, Rass A, Mitsiadis TA, Fried K, Lendahl U, Wroblewski J. Expression of the intermediate filament nestin during rodent tooth development. *Int J Dev Biol.* 1995 Dec;39(6):947-56. PMID: 8901197.
21. Thesleff I, Hurmerinta K. Tissue interactions in tooth development. *Differentiation.* 1981;18(2):75-88. doi: 10.1111/j.1432-0436.1981.tb01107.x. PMID: 7011890.
22. Vidovic-Zdrilic I, Vining KH, Vijaykumar A, Kalajzic I, Mooney DJ, Mina M. FGF2 Enhances Odontoblast Differentiation by α SMA⁺ Progenitors In Vivo. *J Dent Res.*

2018 Sep;97(10):1170-1177. doi: 10.1177/0022034518769827. Epub 2018 Apr 12. PMID: 29649366; PMCID: PMC6169028.

23. Vidovic I, Banerjee A, Fatahi R, Matthews BG, Dymont NA, Kalajzic I, Mina M. α SMA-Expressing Perivascular Cells Represent Dental Pulp Progenitors In Vivo. *J Dent Res*. 2017 Mar;96(3):323-330. doi: 10.1177/0022034516678208. Epub 2016 Nov 13. PMID: 27834664; PMCID: PMC5298392.

4.2 Artigo 2

Mastering dentinogenesis using adjuvant photobiomodulation therapy in murine conservative dental pulp procedures

Abstract

Pericytes and glial cells participate in the tooth regenerative process as the primary sources of stemcells. We previously demonstrated that pericytes and their subpopulations (Nestin+NG2+ and Nestin-NG2+) act as frontline defense cells in short-term dental pulp injury and that photobiomodulation therapy (PBMT) may positively stimulate them. The aim of this study was to examine the effect of PBMT on pericytes subpopulations and neural progenitor stem cells (Nestin+) following dental pulp capping after experimental dental pulp exposure in mice. We compared cell localization and distribution in a Nestin-GFP/NG2-DsRed reporter mice model after dental pulp capping with Mineral Trioxide Aggregate (MTA) associated or not with PBMT, for 7 and 21 days. Pericytes were found to contribute to dental pulp repair in both groups and were predominantly located close to the injury site. The sources of pericytes and neural progenitors were preserved in the specimens treated with MTA/PBMT, with an architecture resembling that of the intact group. However, the MTA group alone showed a medium horn – i.e., nearby the injury site – lacking Nestin+ cells at both 7 and 21 days, along with repopulation of Nestin-NG2+ cells at 21 days. Notably, the PBMT-treated group demonstrated a colorful medium horn, presenting Nestin+, Nestin+NG2+, and Nestin-NG2+ cell populations. Qualitatively, more inflammatory signs and calcifications were observed in the non-photoactivated MTA group compared to the MTA/PBMT group. Gene expression analysis at 21 days showed upregulation of nestin and glial fibrillary acidic protein, downregulation of NG2 and upregulation of odontodifferentiation genes runt-related transcription factor-2 and dentin sialophosphoprotein in the MTA/PBMT group compared to the MTA group, corroborating the histological data. Altogether, while MTA alone promoted dental pulp healing, combining MTA with PBMT preserved dental pulp stem cell sources and enhanced dentinogenesis. The reparative process mastered by PBMT appeared more closely associated with the original tissues, making this therapy a conservative approach for dental pulp capping procedures.

Keywords: Pericytes, photobiomodulation, dentinogenesis, mineral trioxide aggregate.

Introduction

Pulp exposure can occur due to various causes, including iatrogenic factors, deep carious lesions, or trauma. To promote dental pulp recovery, it is crucial to establish a reparative dentin barrier that protects the remaining vital pulp tissue beneath the mineralized structures. It is well-established that the dental pulp contains cells capable of secreting dentin, known as odontoblasts. Odontoblasts lost due to pulp exposure are replaced by newly differentiated odontoblasts-like cells originating from ectomesenchymal cells located in perivascular and neural niches. Their primary function is to produce tertiary dentin (Bleicher, 2014; Feng *et al.*, 2011; Kaukua *et al.*, 2014; Shi, Gronthos, 2003).

Pericytes, which are perivascular cells involved in neoangiogenesis and blood flow regulation, exhibit plasticity and the ability to differentiate into various cell types, including odontoblasts (Birbrair *et al.*, 2013; Feng *et al.*, 2011; Løvschall *et al.*, 2007). Additionally, neural progenitors, such as glial precursors and Schwann cells, constitute a most of the dental pulp stem cells (DPSCs) population involved in odontogenesis, and they may also participate in the dental pulp repair (Bleicher, 2014; Kaukua *et al.*, 2014). Collectively, pericytes and neural progenitor cells constitute distinct populations of ectomesenchymal cells within the dental pulp, capable of differentiating into odontoblasts-like cells, thus contributing to tissue repair in injured teeth (Feng *et al.*, 2011; Kaukua *et al.*, 2014; Vidovic *et al.*, 2017; Vidovic-Zdrilic *et al.*, 2018).

Photobiomodulation therapy (PBMT) elicits photochemical and photobiological effects, such as the generation of free radicals, nitric oxide, adenosine triphosphate (ATP), and cyclic adenosine monophosphate (cAMP), ultimately enhancing energy production and activating signaling pathways that promote stem cell proliferation and differentiation. This initiates a cascade of signaling events to promote tissue regeneration (Arany *et al.*, 2014; Khorsandi *et al.*, 2020). In studies involving mice, PBMT has demonstrated the ability to stimulate the repopulation of root canals by mesenchymal stem cells and their differentiation into odontoblasts, significantly contributing to dental pulp repair (Moreira *et al.*, 2017). In previous study, we demonstrated that PBMT enhances the activation of pericytes and neural progenitors in injured pulps, reducing inflammatory signals, and suggesting their direct involvement in early stages of dental pulp repair (Gomes *et al.*, 2022). In clinical studies, the application of this therapy has shown improvements in the prognosis of permanent

teeth undergoing pulp capping, a conservative procedure that preserves the remaining vital dental pulp (Deng *et al.*, 2016; Alsofi *et al.*, 2022). Despite promising results observed in previous studies, translating these findings into clinical practice has proven challenging, hindering our understanding of the true role of this therapy in pulp regeneration (Bidar *et al.*, 2016; Shigetani *et al.*, 2011; Ferriello *et al.*, 2010).

MTA has emerged as the most promising biomaterial used in dental pulp conservative or regenerative procedures (Pedano *et al.*, 2020; Nie *et al.*, 2021). This biomaterial is widely recognized for its ability to improve the quality of the dentin barrier formed, reduce the inflammatory response, preserve pulp vitality, and induce the regeneration of exposed pulp (Li *et al.*, 2015; Paula, 2018). MTA has demonstrated the capacity to induce the adhesion, migration, and attachment of undifferentiated cells to form a dentin bridge and causing a milder inflammatory effect in dental pulp when compared to calcium hydroxide (Zhu *et al.*, 2014; Zhu *et al.*, 2015). Histological analyses have revealed that the hard tissue formed after dental pulp capping with MTA does not result from the differentiation of true odontoblasts and lacks the properties of regular dentin, suggesting that it is a reparative process rather than true regeneration (Damaschke *et al.*, 2019). In this context, the cellular mechanisms underlying this process require further understanding. Our study investigated the hypothesis that pericytes and neural cells are guided or activated by light to promote dental pulp tissue repair.

Material and Methods

Animal Model

The experiments were performed following the ARRIVE guidelines. Approved by the Animal Care and Use Committee of the Federal University of Minas Gerais (protocol #181/2020). The expected Nestin GFP/NG2 DsRed phenotypes were obtained as previously described (Birbrair *et al.* 2013). All animals were housed under controlled conditions and under a 12:12 hour light-dark cycle and fed *ad libitum*.

In vivo procedures

A total of 48 ten-week-old male or female Nestin GFP/NG2 DsRed mice or wild-type (WT) were used for the histologic (n = 24; n = 6 mice/group) and confocal (n = 24

n = 6 mice/group) analysis of this study. Other 12 WT animals were used for molecular analysis (n = 3 mice/group). A mice dental bed was created by three-dimensional (3D) printing in nylon filament 12 (3D Fortus 380 MC, Stratasys, USA (Gomes *et al.*, 2022)). The experimental pulp exposure on the mice maxillary first molars was performed by removing the superficial enamel with a spherical LN drill (Maillefer, Cotia, SP, Brazil), creating an initial niche in the mesial fossa, followed by the penetration of a K#20 endodontic file until the roof of the pulp chamber was breached. Then, the pulp capping was performed with white Mineral Trioxide Aggregate (MTA) (Angelus, PR, Londrina, BRA) and filled with a photoactivated flow resin (Ivoclar, LI, Switzerland, CHE), according to the manufacturer's instructions. The animals were medicated with analgesic (Meloxicam, 5mg/Kg once a day for 72-h).

Photobiomodulation Therapy (PBMT)

In the MTA/PBMT group, before pulp capping with MTA, the PBMT was performed transoperatively with an indium-gallium-aluminum-phosphide (InGaAlP) customized diode laser, in continuous operation. The dosimetry parameters were as follows: 660 nm, 20 mW, 0.028 cm² spot area, 0.71 W/cm², 7 s, 5 J/cm², 0.14 J total energy per point, in punctual and contact modes (Diniz *et al.*, 2018). Then, the teeth were filled with the photoactivated flow resin. In the next 3 days, PBMT was also performed (24, 48 and 72-h).

Confocal analysis

For confocal analysis, samples were immersed overnight in sucrose 30% (w/v) and then embedded in optimum cutting temperature (OCT) compound. Sections of 20 µm thickness were counterstained with DAPI in mounting medium (Abcam, Cambridge, UK) and analyzed. In vivo tracking of labelled cells in the dental pulp were observed in microscope by using an Eclipse Ti with an LSM 880 confocal head (Zeiss, Oberkochen, Germany). Plan Apo 20x and 40x objectives were used. A scan large image was performed for each sample under the 10x objective. Each channel was counted separately, except for Type 1 and Type 2 pericytes subpopulations that were counted in the merged images. A threshold was manually adjusted, and the fluorescence area (mean gray values) was calculated by using the Fiji software (NIH).

The green (GFP), red (DSRed), and blue (DAPI) channels and their compositions were used to quantify cellular fluorescence in the tissues, serving as markers for neural cells, pericytes, and the classic cellular nucleus, respectively. Furthermore, type II pericytes exhibit yellow fluorescence due to the colocalization of the GFP and DSRed markers.

RT-qPCR

For qPCR analysis, upper first molars and surrounding tissues were obtained in triplicate and subsequently homogenized. Total RNA was extracted using the RNeasy Mini Kit (Qiagen), following the manufacturer's instructions. A total of 1250 ng of RNA was then subjected to reverse transcription using the SuperScript VILO IV Master Mix (Thermo Fisher Scientific). The resulting cDNA was used as the template for subsequent reactions, which employed the SYBR Green PCR Master Mix (Thermo Fisher Scientific). The genes analyzed, along with their respective primer sequences, are listed in Table 1. Relative expression levels were determined by comparing the means of the Ct values obtained from duplicate measurements, normalized to the endogenous control, Glyceraldehyde-3-phosphate dehydrogenase (GAPDH), against a reference sample using the $2^{-\Delta\Delta Ct}$ formula.

Table 1. Primer sequences used for qPCR analysis.

Gene	Primers
NG2	Forward: 5' - CTGTTCTCACACAGAGGAGCC - 3' Reverse: 5' - TGGACAGACGGTCAACTTCC - 3'
Nestin	Forward: 5' - TGGCTACATACAGGACTCTGC - 3' Reverse: 5' - AAGGATGTTGGGCTGAGGAC - 3'
GFAP	Forward 5'-CTTCCCGCAACGCAGAG-3' Reverse 5'-GAGCCGTGGGCACTAAA-3'
CD105	Forward 5'- TGCACCTGGCCTACAATTCCA-3' Reverse 5'- AGCTGCCCACTCAAGGATCT-3'
Dspp	Forward: 5' - CTGGGCCATTCCGGTTCC - 3' Reverse: 5' - ATCTCACTGCCATCTGGGGA - 3'
RUNX-2	Forward: 5' - CAGGCAGGTGCTTCAGAACT - 3' Reverse: 5' - GGGGTGTAGGTAAAGGTGGC - 3'

SDF1- α	Forward: 5' CAGTGACGGTAAACCAGTCAGC - 3' Reverse: 5' - TGGCGATGTGGCTCTCG - 3'
TWIST	Forward: 5' - AGG CCG GAG ACC TAG ATG TCA TT - 3' Reverse: 5' - TTG GTC TCT GCT CTT CTA ATT TCC A
P38	Forward: 5' - TGG ATA TTT GGT CCG TGG GC- 3' Reverse: 5' - TGC TGA AGC TGG TTA ATA TGG TCT - 3'
GAPDH	Forward: 5' - ACGGCCGCATCTTCTTGTGCA - 3' Reverse: 5' - CGCCAAATCCGTTACACCGA - 3'

Histologic analysis

In the 7th or 21st post-operative day, the animals were euthanized, and the specimens were fixed in 4% formaldehyde for 48 hours. Then, samples were demineralized in 10% EDTA for 21-28 days, and paraffin embedding. The blocks were serially sectioned using a microtome at 6 μ m sections (Leica, Wetzlar, Germany) and were either stained for hematoxylin and eosin (H&E) or Masson's Tricome (MT).

For descriptive analysis, ten histological fields of the distal, middle and mesial horns (injured region) of each experimental group were randomly selected and analyzed (400x) as follows: (1) Pulp vitality: total vitality of the coronal dental pulp (++) , partial vitality of the coronal dental pulp (+) and non-vital (-). Pulp with necrotic tissue or absence of tissue within the pulp chamber were considered non-vital, while samples with pulp tissue represented by vascularized connective tissue were vital; (2) Inflammatory signs: only samples classified as vital (++ and +) were evaluated for the condition of the pulp tissue distant from the injury, designated as: presence of only one of the inflammatory signs (+), two signs of inflammation (++) , more than two inflammatory signs (+++), or absence of inflammation (-). The inflammatory signs considered were: dilated and congested blood vessels; red blood cells outside the vessels; infiltration of inflammatory cells (such as polymorphonuclear leukocytes and neutrophils); and microabscesses.

To evaluate the formation of dentin barrier and mineralization in the dental pulp (ABRAHÃO *et al.*, 2006), MT staining was used following the manufacturer's recommendations. For each histological section, three consecutive fields of the crown with 20 and 40x magnification were selected for analysis. All samples were observed under an optical microscope (DM 4000 B, Leica®, Germany) and all histological

analyses were performed by a calibrated and blinded examiner.

Statistical Analysis

After normality test, statistical significance between groups was calculated using one-way ANOVA followed by Tukey's post-hoc using the GraphPad Prism 9.0 Software (GraphPad Software, La Jolla, USA). Data were expressed as means \pm standard error. The differences among the groups were considered significant when $p < 0.05$ in all experiments.

Results

The arrangement of labelled cells in healthy conditions was compared, revealing that NG2-positive cells were more abundantly distributed in the central region, with a small portion occupying the odontoblastic layer in the intact group (Figure 1, A).

In both injured groups maintained for 7 and 21 days, undifferentiated cells (Nestin+) and pericytes (NG2+) increased and migrated towards the injured region. At the 7-day, the MTA group showed necrotic tissue in the middle pulp horn, near the lining material, while in the MTA/PBMT group, these cells were markedly recruited to the injured region (Figure 1, B-C).

Structures suggestive of larger blood vessels are observed in the 7-day MTA group when compared to the MTA/PBMT (Figure 1, B). At 21 days, the MTA group had qualitatively slight and smaller blood vessels compared to the MTA/PBMT group, which appeared to stimulate the enlargement of smaller vessels (Figure 2, H, M, P, S).

Within 21 days, in the non-photoactivated MTA group, pericytes (NG2+) were observed approaching the injured region. In the MTA/PBMT group, not only pericytes but also an increase in the presence of undifferentiated cells co-expressing Nestin/NG2 were observed in this region (Figure 2).

At 7 days, there was a significant increase in the expression of NG2, CD105, SDF-1 α , and Twist genes in the MTA group compared to the MTA/PBMT group, while P38 was significantly increased in MTA/PBMT group (*data not showed*). Gene expression analysis at 21 days showed increased expression of nestin and glial fibrillary acidic protein (GFAP), reduced expression of NG2, and enhanced expression of odontodifferentiation genes, runt-related transcription factor (RUNX)-2 and

Dentin Sialoprophosphoprotein (DSPP) in the MTA/PBMT group compared to the MTA group, thereby corroborating the histological observations (Figure 2).

Masson's Trichrome staining at 7 days did not reveal formation of dentin barrier in either the photoactivated or non-photoactivated groups, although diffuse calcifications were associated with micro vessels in 75% of samples of MTA group in the middle and distal horns (Figure 3).

At 21 days, the presence of a dentin barrier close to the lesion was observed in both groups (Figure 4). In the PBMT/MTA group, calcifications were not observed, and only 33% of the samples showed discrete calcifications without well-defined limits in the middle horn (Figure 5, C, E). Additionally, 75% of the teeth of MTA group presented dentin bridge formation and produced tertiary dentin in an exacerbated manner, reducing the volume of the medial pulp chamber. On the other hand, the MTA/PBMT group showed dentin bridge formation in 33% of the samples, and 66% presented tertiary dentin with a decrease in pulp volume (Figure 4, C, D). Notably, samples from MTA group showed signs of compromised pulp vasculature, with larger caliber vessels and red blood cells protruding from them (Figure 4, C).

The inflammatory process was graded using hematoxylin and eosin staining. Regarding pulp vitality, at 7 days, the MTA group showed total vitality in 50% of the samples, and 50% showed partial vitality. In the MTA/PBMT group, 66% maintained total vitality and 33% partial vitality. As for inflammatory signs, the MTA group showed two inflammatory signs in 83.33% of the samples and 16.66% showed at least one sign. Photoactivated samples showed three inflammatory signs in 33.33%, 33.33% showed two inflammatory signs, and 33.33% were not inflamed (Figure 5).

At 21 days, in MTA group, 60% of the samples retained total vitality, and 40% with partial vitality. In the photoactivated samples, 80% maintained total vitality, while 20% showed partial vitality (Figure 6).

At least one inflammatory sign was observed in 100% of the MTA group samples, whereas 60% of the photoactivated samples showed no inflammatory signs. Tertiary dentin was observed in 100% of the samples in both non-photoactivated and photoactivated groups, concentrated in the middle third of the dental pulp. A total dentin bridge was present in 40% of the MTA group samples and in 60% of the photoactivated group, with 20% presenting partial dentin bridge in the photoactivated group.

Among the inflammatory signs, the presence of large caliber vessels, congested and with erythrocytes protruding from them, was prominent in 60% of MTA group

samples and was observed in 20% of the photoactivated group samples (Figure 6).

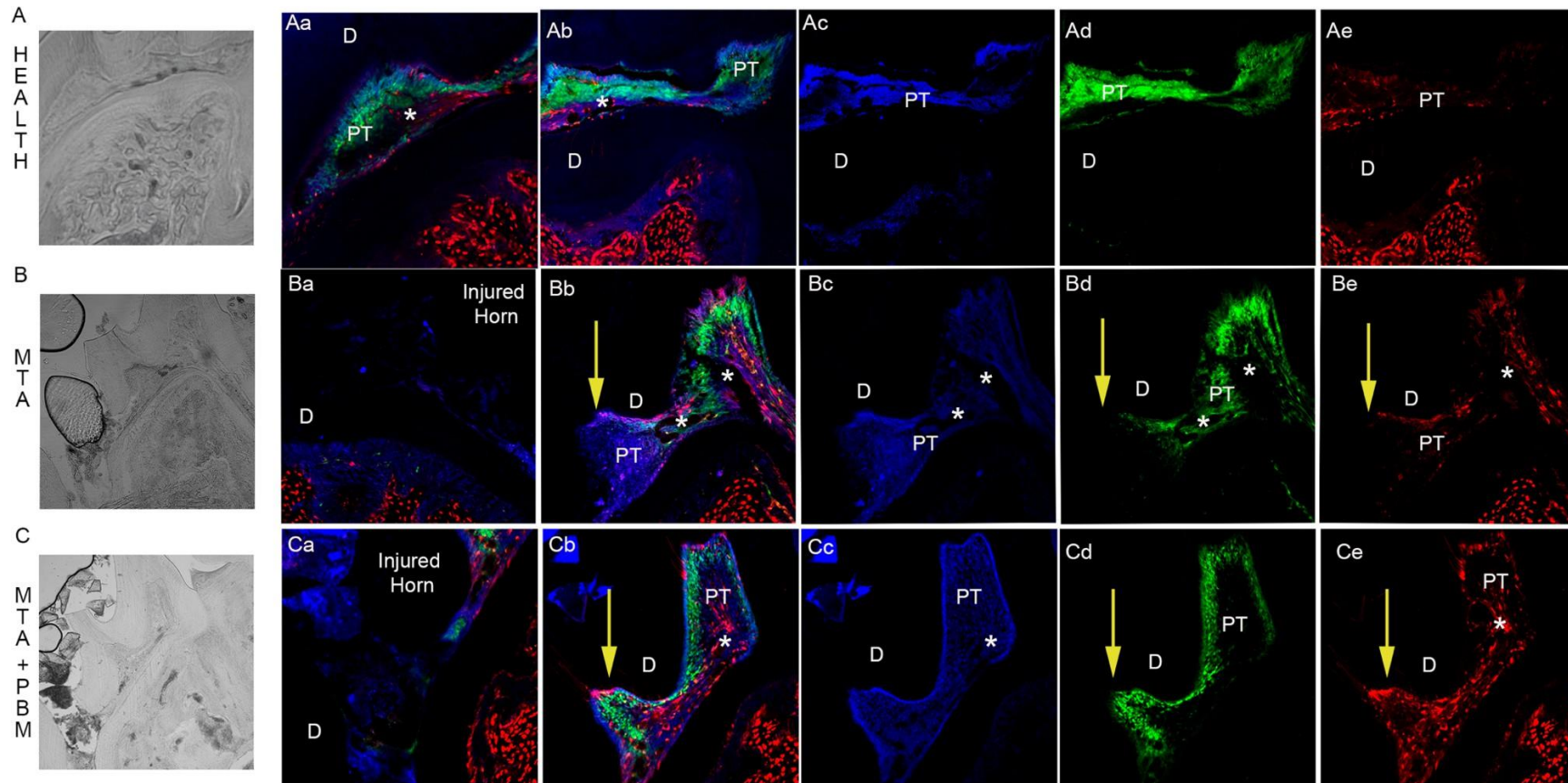


Figure 1 Analysis of pericytes and neural cells in healthy tissues and after injury treated with MTA and MTA+PBMT for 7 days. We have representative sagittal images of first molars from mice at a 20x magnification. Images in bright-field, merge between fluorescence (DAPI, Nestin/GFP, and NG2/DsRed), and individual fluorescence channels are presented in this order. The first section (A, Aa, Ab, Ac, Ad, Ae) depicts an intact tooth, where we observe the presence of NG2-positive cells represented by red fluorescence scattered in the central region of the dental pulp (PT) (Ae) and discretely in the odontoblastic layer (Aa). Meanwhile, neural cells are represented by green fluorescence and are organized in the outermost layer of the PT. In the second section (B, Ba, Bb, Bc, Bd, and Be), we have a tooth injured in its mesial horn (Ba). We observe NG2 cells prominently expressed in the region distant from the injured area and in the odontoblastic layer (Bd, Be). Neural-origin cells maintain their characteristic peripheral location in the pulp tissue but move away from the injured region (Bd). In the third section, we observe an injured tooth treated with MTA+PBMT. Note that the overexpressed NG2-positive cells are very close to the injured region as well as in the odontoblastic layer (Cb, Ce), and neural cells are also in proximity to the injured tissue (Cd).

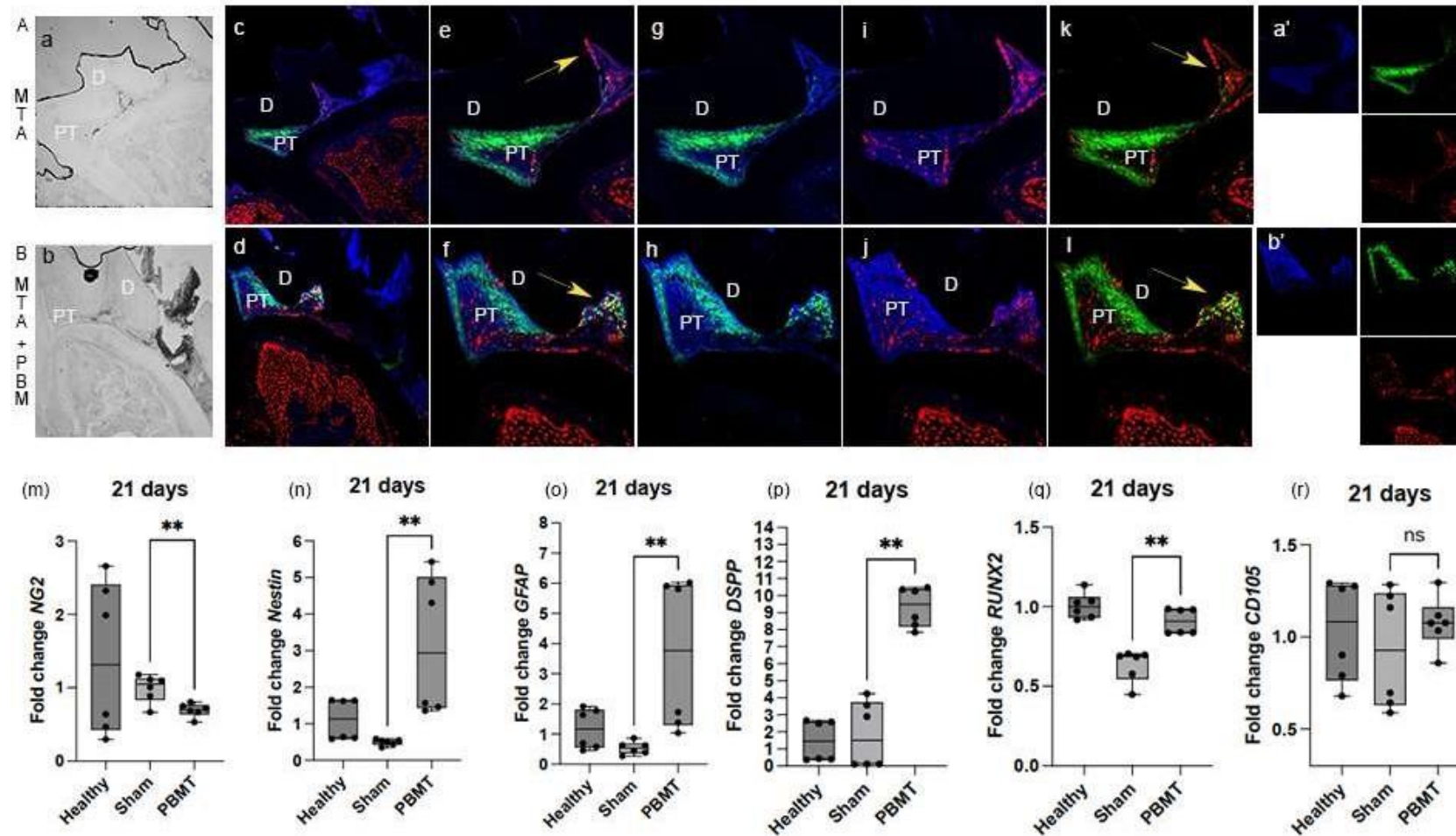


Figure 2 - Analysis of pericytes and neural cells in healthy tissues and after injury treated with MTA and MTA+PBMT for 21 days. Two teeth with sagittal sections, one treated with MTA and the other with PBMT after 21 days, are represented here. (a) Representative sections in bright-field (A and B) and epifluorescence. Note some NG2-positive cells in the odontoblastic layer and near the injured region treated with MTA alone (yellow arrows) (e and k) and the reduced distribution of Nestin-positive cells near the injury site (g). In the MTA+PBMT-treated group, cells with co-markers for Nestin and NG2 are present in the region near the injury (yellow arrows) (f, l), and Nestin+ cells are also recruited to the injured region (h). Molecular analyses of genes (m) NG2, (n) Nestin, (o) GFAP, (p) Dspp, (q) RUNX2, (r) CD105 in intact and MTA and MTA+PBMT-treated groups. Data are shown as mean \pm SEM, $n = 3$ for each group. Student t -test or Mann-Whitney. * $p < 0.05$. NS, not significant; D, dentin; PT, pulp tissue; AB, alveolar bone.

Dental Pulp - Treatment for 07days

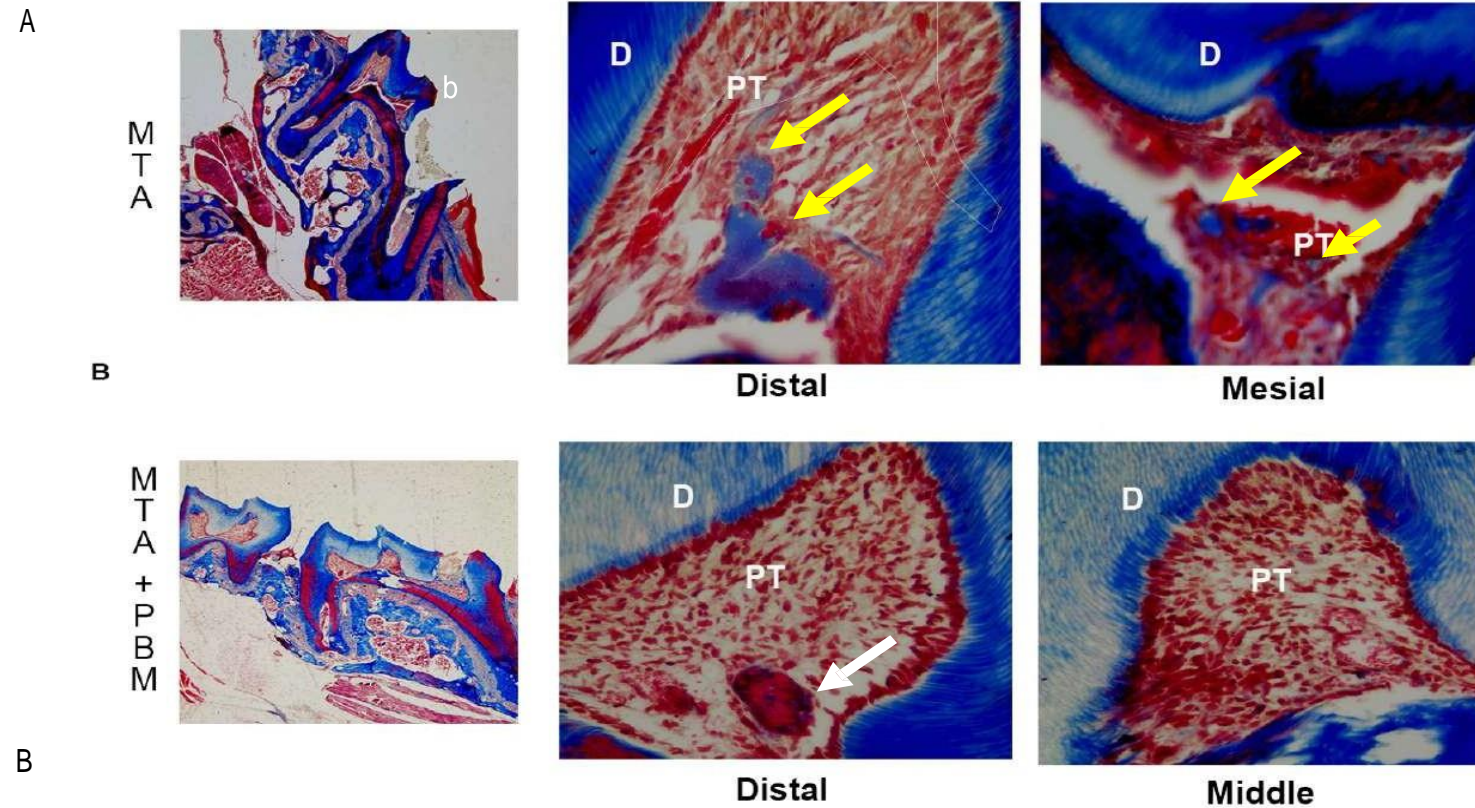


Figure 3- Analysis of mineralization in dental pulp after capping with MTA or photoactivated MTA after 7 days. Representative images of mineralization analysis. (A-B) (10x). Panoramic microscopic appearance of dental pulp in the middle and distal thirds after pulp capping with MTA and MTA+PBMT. Extensive diffuse calcifications without well-defined boundaries observed in the pulp treated with MTA in the mesial and distal horns (Yellow arrows). In contrast, we observed discrete mineralization around blood vessels in the MTA+PBMT group (White arrows). Masson's trichrome, 40x.

Dental Pulp - Treatment for 21 days

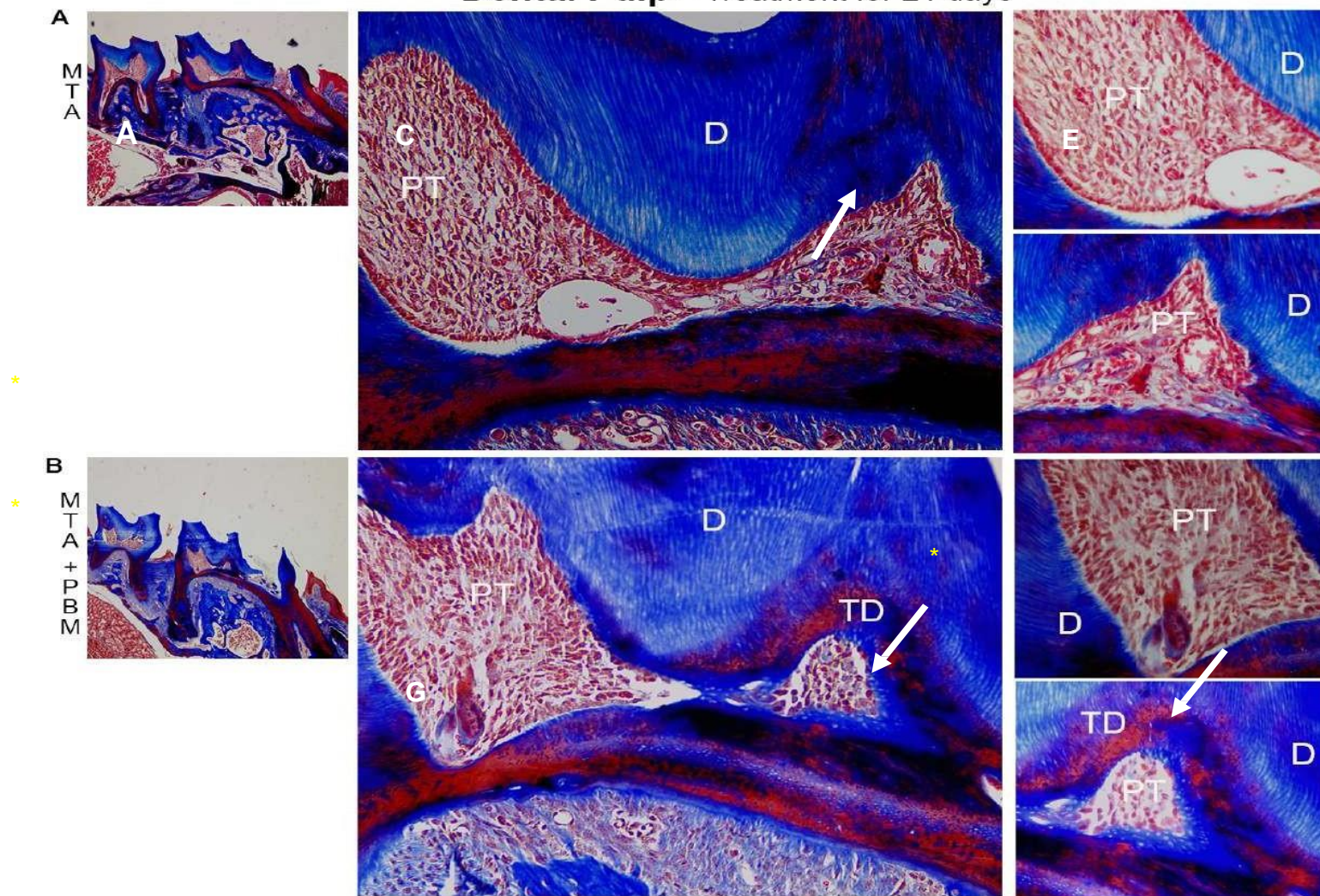


Figure 4 - Analysis of mineralization in dental pulp after treatment with MTA and photoactivated MTA after 21 days. Representative images of mineralization analysis. (A-B) (10x). Panoramic microscopic appearance of dental pulp in the middle and distal thirds after pulp capping with MTA and MTA+PBMT (20x). Note the presence of tertiary dentin in both treatments, highlighted by white arrows (C, D, F, H). Inflammatory signs such as congested blood vessels are observed more frequently in the MTA group (*) (c). Presence of collagen fibers stained in red in the tertiary dentin of the photoactivated group is observed, indicating a more recent stage of dentin mineralization in the PBMT group (H) (40x) Masson's trichrome.

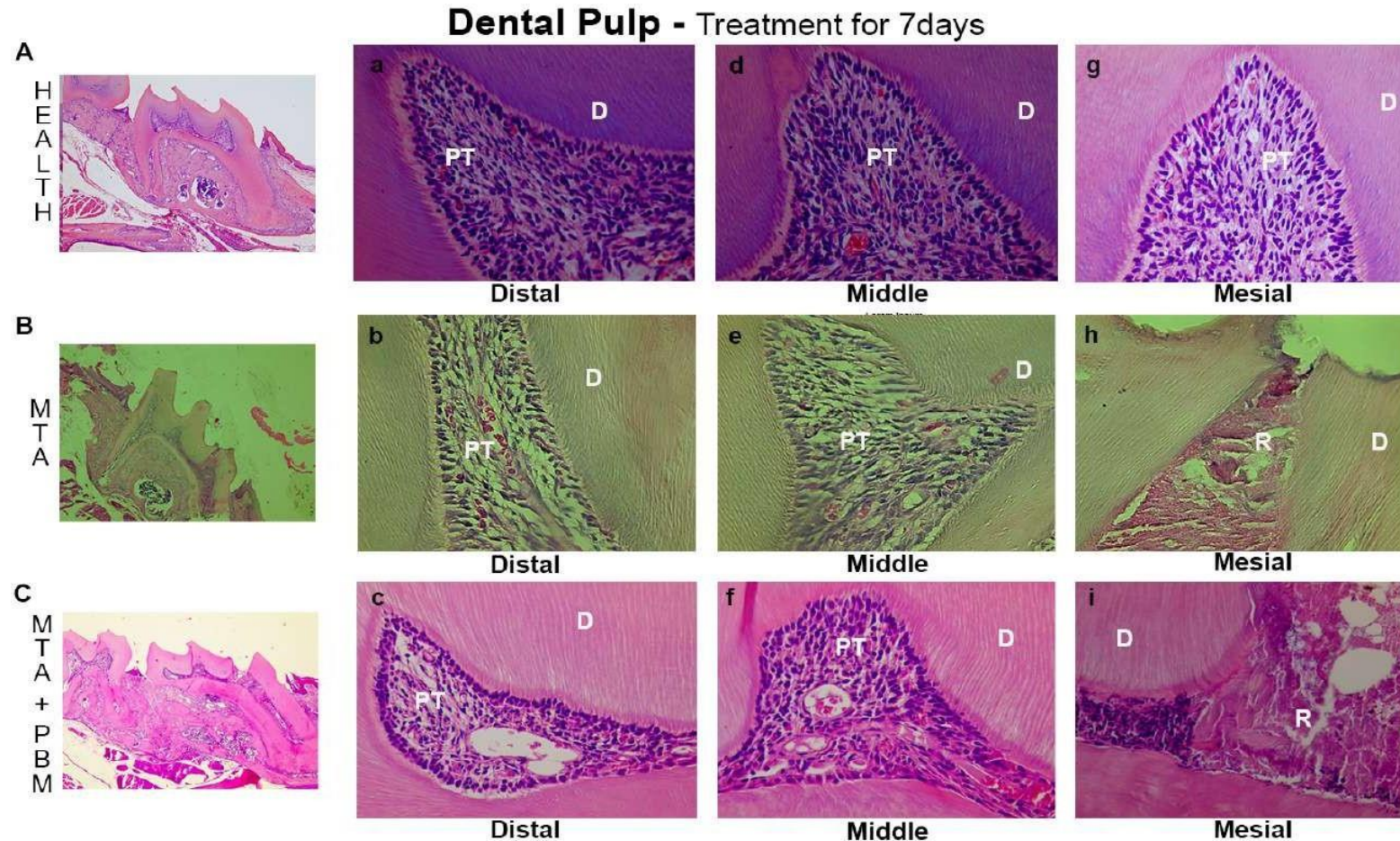


Figure 5 Analysis of inflammatory signs after treatment with mta and photoactivated mta in 7 days. Histological evaluation of pulp vitality signs and inflammatory signs. (a) Representative photomicrographs showing sagittal sections of an upper first molar from the intact group. The horns exhibit highly cellularized connective tissue with vessels of varying diameters and congestion. (b) Representative photomicrographs showing sagittal sections of an upper first molar injured and treated with MTA. (h) The mesial horn shows the restorative material, (e) the middle horn demonstrates the presence of inflamed pulp tissue with inflammatory infiltrate and small-caliber blood vessels observed in this region, while in the distal horn, we observe congested larger-caliber vessels. (C) Dental pulps exposed and treated with MTA+PBMT show that the (i) mesial horn presents the restorative material; (f) in the middle third, we observe inflamed connective tissue with infiltration of inflammatory cells and congested larger-volume blood vessels, but the odontoblastic layer is maintained, and (c) in the distal horn, we observe congested larger-caliber blood vessels. D, Dentin; PT, pulp tissue; R, Restorative Material. Hematoxylin and Eosin 40x.

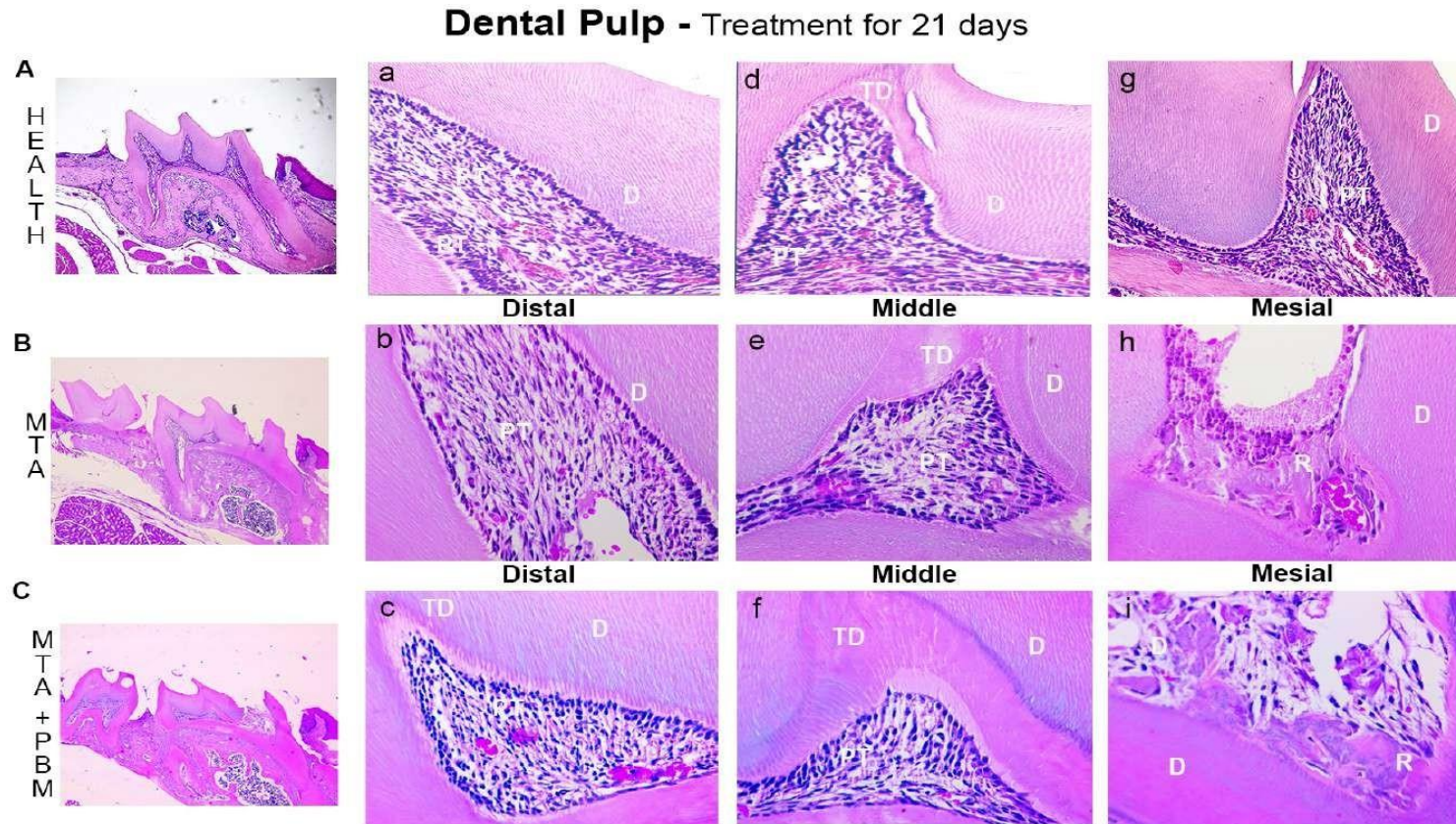


Figure 6 - Analysis of inflammatory signs after treatment with mta and photoactivated mta in 21 days. Histological evaluation of inflammatory signs and mineralized tissue formation. (a) Representative photomicrographs showing sagittal sections of an upper first molar from the intact group. The horns exhibit highly cellularized connective tissue with vessels of varying diameters and congestion. (B) Representative photomicrographs showing sagittal sections of an upper first molar treated with MTA. The distal horn presents swollen connective tissue with infiltration of mononuclear inflammatory cells and many congested vessels. The middle horn shows an intense mononuclear inflammatory infiltrate, a reduction in the pulp chamber volume due to the presence of dentin, and small areas of necrosis. The mesial horn displays the restorative material maintained in the cavity. (c) Dental pulps exposed and treated with MTA+PBM show that the distal horn exhibits characteristics similar to those described for the intact group, with an important detail being the presence of an additional layer of dentin with a lighter color not observed in the previous groups, smaller blood vessels are observed and congested. The middle horn contains preserved dental pulp with its volume reduced by the dentin, also demonstrating a thin layer of dentin that is lighter than that shown in the previous groups. The mesial horn presents the restorative material. D, Dentin; PT, pulp tissue; TD, Tertiary Dentin.

Discussion

Pericytes and neural-origin cells serve as a source of stem cells in pulp tissue regeneration (Shi, Gronthos, 2003; Feng, *et al.*, 2011; Kaukua, *et al.*, 2014; Gomes *et al.*, 2022). We have previously demonstrated that pericytes and their subpopulations present in the pulp are positively influenced by PBMT during the early stages of pulp inflammation in injured pulps without any treatment, maintaining the viability of these cells and creating a favorable microenvironment for dentin-pulp complex regeneration in a short period of time (Gomes *et al.*, 2022). In this study, we examined the localization and distribution of these cells in a mice model after 7 and 21 days following pulp capping with MTA associated or no with PBMT. After 7 and 21 days, we observed that the sources of pericytes and neural progenitor cells were preserved in the samples treated with PBMT/MTA and exhibited a disposition similar to the uninjured control group. However, in the group that received only MTA, we identified a central area - near the injury - with a scarcity of Nestin+ cells at 7 and 21 days, along with a recurrence of Nestin-NG2+ cells at 21 days. On the other hand, the PBMT-treated group revealed a central area containing components of Nestin+, Nestin+NG2+, and Nestin-NG2+ cell populations. Noteworthy, Nestin, in addition to being a marker of undifferentiated cells, is also an odontoblast marker (Terling *et al.*, 1995), and this result is suggestive.

Previous studies support the appropriateness of a 660 nm wavelength laser for stimulating dental pulp stem cells (Eduardo *et al.*, 2008; Pereira *et al.*, 2012; Zaccara *et al.*, 2015; Soares *et al.*, 2015; Neto *et al.*, 2016). However, variations in application modalities and total energy doses hinder the standardization of effective PBMT protocols (Borzabadi-Farah *et al.*, 2016). To assess the modulatory effect of irradiation on dental pulp, we adopted an approach previously developed in earlier studies with dental pulp cells, where this treatment resulted in proliferation and increased mineralization of dental pulp cells under different experimental conditions (Moreira *et al.*, 2017; Diniz *et al.*, 2018; Ferreira *et al.*, 2018; Gomes *et al.*, 2022). It has been demonstrated the possibility of performing pulp capping using low-intensity laser in mice teeth, resulting in stimulated transforming growth factor (TGF)- β 1, which in turn induced stem cell differentiation and dental pulp regeneration (Arany *et al.*, 2014).

PBMT establishes itself as a reliable treatment for dental pulp (Meza *et al.*, 2018; Marques *et al.*, 2016), demonstrating the ability to induce the differentiation of mesenchymal stem cells (MSCs) into odontoblasts (Abdelgawad *et al.*, 2021; Yang *et al.*, 2023). Remarkably, a subpopulation of PBMT-susceptible MSCs has neural origins and corresponds to pericytes (Gomes, *et al.*, 2022). The expression of Nestin+ characterizes neural progenitor cells, which exhibit notable plasticity and the ability to differentiate into functional neurons and glial cells (Widera, 2009). Several studies attest to the beneficial effect of PBMT on glial cells (Huang, 2015; Wang, 2021) and its ability to stimulate neurogenesis (Wu, 2021). In this context, we observed a positive regulation of the Nestin gene in the groups treated with PBM at advanced stages of the pulp regeneration process.

Previous studies have delineated the existence of two subpopulations of pericytes in a transgenic model doubly positive for NG2 and Nestin in muscle, neural, angiogenic, and adipogenic tissues (Birbrair *et al.*, 2013, 2014). In dental pulp, these NG2+ cells were termed type I pericytes, which predominate during the early stages of inflamed pulp, while NG2+Nestin+ type II cells are observed more discretely (Gomes *et al.*, 2022). In the present study, conducted over a longer experimental period to evaluate pulp regeneration, we observed the presence of type I pericytes near the injured area compared to the control group, accompanied by a positive regulation of the NG2 gene at the onset of pulp inflammation, consistent with the literature's evidence. Furthermore, we identified cells with dual labeling for neural progenitors and pericytes, Nestin+NG2+, near the dentin barrier at advanced stages of pulp regeneration, suggesting that type II pericytes may be in a more advanced stage of differentiation, which is consistent with the results obtained in this study.

Tertiary dentin can also be observed in teeth that have undergone wear and damage. This dentin is a response mechanism, leading to the formation of sclerotic tissue that reduces dentin permeability. This response serves as a defense that protects the dental pulp against harmful irritations (Nudel *et al.*, 2021; Trostand *et al.*, 1971). The formation of tertiary dentin is expected when a bioactive material is applied directly to the exposed or partially removed dental pulp (in procedures such as direct pulp capping and pulpotomy) (Tran *et al.*, 2019; Nowicka *et al.*, 2013). In this study, we examined the formation of tertiary dentin after experimental injuries treated with MTA with and without photoactivation. The formation of dentin or mineralization of dental pulp raises questions about the quality of the resulting tissue. Often, this

mineralization is of a scar-like nature and does not represent true tissue regeneration, exhibiting characteristics of osteodentin that differ from the original dentin (Dammasche *et al.*, 2019; Nudel *et al.*, 2021; Yoon *et al.*, 2021). This type of atypical repair can contain various regenerative components but may also increase the risk of uncontrolled pulp inflammation and necrosis (Gurtner *et al.*, 2008; Kunert *et al.*, 2015). In our study, we observed the formation of a mineral barrier in both groups. However, the group treated with MTA without photoactivation exhibited a higher occurrence of diffuse calcifications and mineral nodules distributed in the dental pulp, along with a greater presence of long-term inflammatory signs, as evidenced by histological analyses.

Previous studies have shown that pericytes can give rise to DSPP+ odontoblasts and BSP+ osteoblasts in reparative dentin (Vidovic *et al.*, 2017). The DSPP gene, crucial for dentin mineralization and dental development, exhibited positive regulation at advanced stages of pulp regeneration in the photoactivated group compared to the non-photoactivated group, indicating similarities with neoformed dentin and the original tissue (Lee *et al.*, 2012; Chen *et al.*, 2015; Lim, 2021). Similarly, the RUNX-2 gene, essential for tooth formation and odontoblast differentiation, also showed positive regulation in the photoactivated group. The upregulation of RUNX-2, DSPP, Nestin, and GFAP in the PBMT-treated group confirms the influence of PBMT on neural cells, stimulating their odontoblastic phenotype during dental pulp repair (Camilleri, 2006; Cohen, 2009; Chen, 2016).

Single-cell RNA sequencing studies from public datasets have unveiled a broader correlation within specific perivascular cell expression patterns and attempted to differentiate Nestin+NG2+ and Nestin-NG2+ subpopulations (Gomes *et al.*, 2022). Indeed, the investigated genes associated with stem cell differentiation or terminal odontoblast differentiation exhibited highly similar expression profiles between Nestin (NES) and NG2 (Cspg4) genes. Nevertheless, nestin expression significantly overlapped with the expression of certain transcription factors relevant to mesenchymal stem cell maintenance and cell cycle control, such as Twist1 and BZW (Li *et al.*, 2009; Meng *et al.*, 2015). Conversely, the expression of RUNX-2, Mapk1, and Acta2 (α -SMA) showed a deeper correlation with Cspg4 than the nestin gene. RUNX-2 plays a role in determining the cellular fate (osteogenic vs. dentinogenic lineage) of mesenchymal progenitors in dental pulp (Vijaykumar *et al.*, 2020). Twist1, on the other hand, stimulates DSPP promoter activity by antagonizing

RUNX-2 function in pulp cells (Li *et al.*, 2011). Consequently, Twist1 is likely required for the final events that drive odontoblast differentiation, leading to the subsequent deposition of the primary dentin matrix (Li *et al.*, 2011). Our results herein demonstrated a correlation between the upregulation of Nestin, DSPP, and RUNX-2 genes in the PBMT-treated groups, suggesting that this therapy stimulated these cells' commitment to odontoblastic potential after an extended experimental period, along with evidence of dentin barrier formation.

Correlating the formation of mineral nodules in other undesired areas of dental pulp, along with the absence of Nestin⁺ cells in the region near the injury during the early stages and a reduced presence in the advanced stages of pulp repair, associated with the upregulation of inflammatory genes, such as SDF1- α , in the early stages and the downregulation of odontogenic phenotype genes in the advanced stages of repair, MTA appear to induce this atypical pulp repair. In contrast, PBMT seems to provide a pulp regeneration and dentin barrier formation more similar to healthy tooth tissue. This is attributed to the presence of the dentin barrier in the region of the injury with a lower quantity of inflammatory signals and positively regulated odontoblastic genes, along with an increase in Nestin⁺, Nestin⁺NG2⁺ cells in the region near the injury in both the early and advanced stages of pulp repair.

REFERENCES

1. Abdelgawad L, Salah N, Sabry D, Abdelgwad M. Efficacy of Photobiomodulation and Vitamin D on Odontogenic Activity of Human Dental Pulp Stem Cells. *J Lasers Med Sci*. 2021 Jun 24;12:e30. doi: 10.34172/jlms.2021.30. PMID: 34733753; PMCID: PMC8558714.
2. Alsofi L, Khalil W, Binmadi NO, Al-Habib MA, Alharbi H. Pulpal and periapical tissue response after direct pulp capping with endosequence root repair material and low-level laser application. *BMC Oral Health*. 2022 Mar 4;22(1):57. doi: 10.1186/s12903-022-02099-0. PMID: 35246103; PMCID: PMC8895576.
3. Arany PR, Cho A, Hunt TD, Sidhu G, Shin K, Hahm E, Huang GX, Weaver J, Chen AC, Padwa BL, Hamblin MR, Barcellos-Hoff MH, Kulkarni AB, J Mooney D. Photoactivation of endogenous latent transforming growth factor- β 1 directs dental stem cell differentiation for regeneration. *Sci Transl Med*. 2014 May 28;6(238):238ra69. doi: 10.1126/scitranslmed.3008234. PMID: 24871130; PMCID: PMC4113395.
4. Bidar M, Moushekhian S, Gharechahi M, Talati A, Ahrari F, Bojarpour M. The Effect of Low Level Laser Therapy on Direct Pulp Capping in Dogs. *J Lasers Med Sci*. 2016 Summer;7(3):177-183. doi: 10.15171/jlms.2016.31. Epub 2016 Jul 18. PMID: 28144439; PMCID: PMC5262485.
5. Birbrair A, Zhang T, Wang ZM, Messi ML, Mintz A, Delbono O. Type-1 pericytes participate in fibrous tissue deposition in aged skeletal muscle. *Am J Physiol Cell Physiol*. 2013 Dec 1;305(11):C1098-113. doi: 10.1152/ajpcell.00171.2013. Epub 2013 Sep 25. PMID: 24067916; PMCID: PMC3882385.
6. Birbrair A, Zhang T, Wang ZM, Messi ML, Mintz A, Delbono O. Pericytes: multitasking cells in the regeneration of injured, diseased, and aged skeletal muscle. *Front Aging Neurosci*. 2014 Sep 18;6:245. doi: 10.3389/fnagi.2014.00245. PMID: 25278877; PMCID: PMC4166895.
7. Bleicher F. Odontoblast physiology. *Exp Cell Res*. 2014 Jul 15;325(2):65-71. doi: 10.1016/j.yexcr.2013.12.012. Epub 2013 Dec 18. PMID: 24361392.
8. Borzabadi-Farahani A. Effect of low-level laser irradiation on proliferation of human dental mesenchymal stem cells; a systemic review. *J Photochem Photobiol B*. 2016 Sep;162:577-582. doi: 10.1016/j.jphotobiol.2016.07.022. Epub 2016 Jul 25. PMID: 27475781.
9. Camilleri S, McDonald F. Runx2 and dental development. *Eur J Oral Sci*. 2006 Oct;114(5):361-73. doi: 10.1111/j.1600-0722.2006.00399.x. PMID: 17026500.
10. Chen Y, Zhang Y, Ramachandran A, George A. DSPP Is Essential for Normal Development of the Dental-Craniofacial Complex. *J Dent Res*. 2016 Mar;95(3):302-10. doi: 10.1177/0022034515610768. Epub 2015 Oct 26. PMID: 26503913; PMCID: PMC4766953.

11. Chen S, Gu TT, Sreenath T, Kulkarni AB, Karsenty G, MacDougall M. Spatial expression of Cbfa1/Runx2 isoforms in teeth and characterization of binding sites in the DSPP gene. *Connect Tissue Res.* 2002;43(2-3):338-44. doi: 10.1080/03008200290000691. PMID: 12489178.
12. Cohen MM Jr. Perspectives on RUNX genes: an update. *Am J Med Genet A.* 2009 Dec;149A(12):2629-46. doi: 10.1002/ajmg.a.33021. PMID: 19830829.
13. Deng Y, Zhu X, Zheng D, Yan P, Jiang H. Use of laser in direct pulp capping: a meta-analysis. *JADA.* 2016 Sep;147(9):935-942
14. Diniz IMA, Carreira ACO, Sipert CR, Uehara CM, Moreira MSN, Freire L, Pelissari C, Kossugue PM, de Araújo DR, Sogayar MC, Marques MM. Photobiomodulation of mesenchymal stem cells encapsulated in an injectable rhBMP4-loaded hydrogel directs hard tissue bioengineering. *J Cell Physiol.* 2018 Jun;233(6):4907-4918. doi: 10.1002/jcp.26309. Epub 2018 Jan 15. PMID: 29215714.
15. Eduardo Fde P, Bueno DF, de Freitas PM, Marques MM, Passos-Bueno MR, Eduardo Cde P, Zatz M. Stem cell proliferation under low intensity laser irradiation: a preliminary study. *Lasers Surg Med.* 2008 Aug;40(6):433-8. doi: 10.1002/lsm.20646. PMID: 18649378.
16. Feng J, Mantesso A, De Bari C, Nishiyama A, Sharpe PT. Dual origin of mesenchymal stem cells contributing to organ growth and repair. *Proc Natl Acad Sci U S A.* 2011 Apr 19;108(16):6503-8. doi: 10.1073/pnas.1015449108. Epub 2011 Apr 4. PMID: 21464310; PMCID: PMC3081015.
17. Ferreira LS, Diniz IMA, Maranduba CMS, Miyagi SPH, Rodrigues MFSD, Moura-Netto C, Marques MM. Short-term evaluation of photobiomodulation therapy on the proliferation and undifferentiated status of dental pulp stem cells. *Lasers Med Sci.* 2019 Jun;34(4):659-666. doi:10.1007/s10103-018-2637-z. Epub 2018 Sep 24. PMID: 30250986.
18. Gomes NA, do Valle IB, Gleber-Netto FO, Silva TA, Oliveira HMC, de Oliveira RF, Ferreira LAQ, Castilho LS, Reis PHRG, Prazeres PHDM, Menezes GB, de Magalhães CS, Mesquita RA, Marques MM, Birbrair A, Diniz IMA. Nestin and NG2 transgenes reveal two populations of perivascular cells stimulated by photobiomodulation. *J Cell Physiol.* 2022 Apr;237(4):2198- 2210. doi: 10.1002/jcp.30680. Epub 2022 Jan 17. PMID: 35040139.
19. Gurtner GC, Werner S, Barrandon Y, Longaker MT. Wound repair and regeneration. *Nature.* 2008 May 15;453(7193):314-21. doi: 10.1038/nature07039. PMID: 18480812.
20. Huang YY, Nagata K, Tedford CE, Hamblin MR. Low-level laser therapy (810 nm) protects primary cortical neurons against excitotoxicity in vitro. *J Biophotonics.* 2014 Aug;7(8):656- 64. doi: 10.1002/jbio.201300125. Epub 2013 Oct 15. PMID: 24127337; PMCID: PMC4057365.

21. Kaukua N, Shahidi MK, Konstantinidou C, Dyachuk V, Kaucka M, Furlan A, An Z, Wang L, Hultman I, Ahrlund-Richter L, Blom H, Brismar H, Lopes NA, Pachnis V, Suter U, Clevers H, Thesleff I, Sharpe P, Ernfors P, Fried K, Adameyko I. Glial origin of mesenchymal stem cells in a tooth model system. *Nature*. 2014 Sep 25;513(7519):551-4. doi:10.1038/nature13536. Epub 2014 Jul 27. PMID: 25079316.
22. Khorsandi K, Hosseinzadeh R, Abrahamse H, Fekrazad R. Biological Responses of Stem Cells to Photobiomodulation Therapy. *Curr Stem Cell Res Ther*. 2020;15(5):400-413. doi: 10.2174/1574888X15666200204123722. PMID: 32013851.
23. Løvschall H, Giannobile WV, Somerman MJ, Jin, et al. Stem cells and regeneration of injured dental tissue. In: *Textbook and Color Atlas of Traumatic Injuries to the Teeth*. Andreasen JO, Andreasen FM, Anderson L, editors Blackwell Pub Professional, 2007.
24. Moreira MS, Diniz IM, Rodrigues MF, de Carvalho RA, de Almeida Carrer FC, Neves II, Gavini G, Marques MM. In vivo experimental model of orthotopic dental pulp regeneration under the influence of photobiomodulation therapy. *J Photochem Photobiol B*. 2017 Jan;166:180-186. doi: 10.1016/j.jphotobiol.2016.11.022. Epub 2016 Dec 2. PMID: 27927605.
25. Lim D, Wu KC, Lee A, Saunders TL, Ritchie HH. DSPP dosage affects tooth development and dentin mineralization. *PLoS One*. 2021 May 26;16(5):e0250429. doi:10.1371/journal.pone.0250429. PMID: 34038418; PMCID: PMC8153449.
26. Meng T, Huang Y, Wang S, Zhang H, Dechow PC, Wang X, Qin C, Shi B, D'Souza RN, Lu Y. Twist1 Is Essential for Tooth Morphogenesis and Odontoblast Differentiation. *J Biol Chem*. 2015 Dec 4;290(49):29593-602. doi: 10.1074/jbc.M115.680546. Epub 2015 Oct 20. PMID: 26487719; PMCID: PMC4705958.
27. Meza G, Urrejola D, Saint Jean N, Inostroza C, López V, Khoury M, Brizuela C. Personalized Cell Therapy for Pulpitis Using Autologous Dental Pulp Stem Cells and Leukocyte Platelet-rich Fibrin: A Case Report. *J Endod*. 2019 Feb;45(2):144-149. doi: 10.1016/j.joen.2018.11.009. PMID: 30711169.
28. Moura-Netto C, Ferreira LS, Maranduba CM, Mello-Moura ACV, Marques MM. Low-intensity laser phototherapy enhances the proliferation of dental pulp stem cells under nutritional deficiency. *Braz Oral Res*. 2016 May 31;30(1):S1806-83242016000100265. doi: 10.1590/1807-3107BOR-2016.vol30.0080. PMID: 27253140.
29. Nie E, Yu J, Jiang R, Liu X, Li X, Islam R, Alam MK. Effectiveness of Direct Pulp Capping Bioactive Materials in Dentin Regeneration: A Systematic Review. *Materials (Basel)*. 2021 Nov 11;14(22):6811. doi: 10.3390/ma14226811. PMID: 34832214; PMCID: PMC8621741.
30. Nowicka A, Lipski M, Parafiniuk M, Sporniak-Tutak K, Lichota D, Kosierkiewicz

A, Kaczmarek W, Buczkowska-Radlińska J. Response of human dental pulp capped with biodentine and mineral trioxide aggregate. *J Endod.* 2013 Jun;39(6):743-7. doi: 10.1016/j.joen.2013.01.005. Epub 2013 Apr 10. PMID: 23683272.

31. Nudel I, Pokhojaev A, Bitterman Y, Shpack N, Fiorenza L, Benazzi S, Sarig R. Secondary Dentin Formation Mechanism: The Effect of Attrition. *Int J Environ Res Public Health.* 2021 Sep 22;18(19):9961. doi: 10.3390/ijerph18199961. PMID: 34639261; PMCID: PMC8507651.

32. Paula AB, Laranjo M, Marto CM, Paulo S, Abrantes AM, Casalta-Lopes J, Marques-Ferreira M, Botelho MF, Carrilho E. Direct Pulp Capping: What is the Most Effective Therapy?- Systematic Review and Meta-Analysis. *J Evid Based Dent Pract.* 2018 Dec;18(4):298-314. doi: 10.1016/j.jebdp.2018.02.002. Epub 2018 Feb 15. PMID: 30514444.

33. Pereira LO, Longo JP, Azevedo RB. Laser irradiation did not increase the proliferation or the differentiation of stem cells from normal and inflamed dental pulp. *Arch Oral Biol.* 2012 Aug;57(8):1079-85. doi: 10.1016/j.archoralbio.2012.02.012. Epub 2012 Apr 1. PMID: 22469390.

34. Pedano MS, Li X, Yoshihara K, Landuyt KV, Van Meerbeek B. Cytotoxicity and Bioactivity of Dental Pulp-Capping Agents towards Human Tooth-Pulp Cells: A Systematic Review of In-Vitro Studies and Meta-Analysis of Randomized and Controlled Clinical Trials. *Materials (Basel).* 2020 Jun 12;13(12):2670. doi: 10.3390/ma13122670. PMID: 32545425; PMCID: PMC7345102.

35. Shigetani Y, Sasa N, Suzuki H, Okiji T, Ohshima H. GaAlAs laser irradiation induces active tertiary dentin formation after pulpal apoptosis and cell proliferation in rat molars. *J Endod.* 2011 Aug;37(8):1086-91. doi: 10.1016/j.joen.2011.05.020. PMID: 21763899.

36. Shi S, Gronthos S. Perivascular niche of postnatal mesenchymal stem cells in human bone marrow and dental pulp. *J Bone Miner Res.* 2003 Apr;18(4):696-704. doi: 10.1359/jbmr.2003.18.4.696. PMID: 12674330.

37. Soares DM, Ginani F, Henriques ÁG, Barboza CA. Effects of laser therapy on the proliferation of human periodontal ligament stem cells. *Lasers Med Sci.* 2015 Apr;30(3):1171-4. doi: 10.1007/s10103-013-1436-9. Epub 2013 Sep 7. PMID: 24013624.

38. Terling C, Rass A, Mitsiadis TA, Fried K, Lendahl U, Wroblewski J. Expression of the intermediate filament nestin during rodent tooth development. *Int J Dev Biol.* 1995 Dec;39(6):947-56. PMID: 8901197.

39. Vidovic-Zdrilic I, Vining KH, Vijaykumar A, Kalajzic I, Mooney DJ, Mina M. FGF2 Enhances Odontoblast Differentiation by α SMA⁺ Progenitors In Vivo. *J Dent Res.* 2018 Sep;97(10):1170-1177. doi: 10.1177/0022034518769827. Epub 2018 Apr 12. PMID: 29649366; PMCID: PMC6169028.

40. Vidovic I, Banerjee A, Fatahi R, Matthews BG, Dymont NA, Kalajzic I, Mina M. α SMA- Expressing Perivascular Cells Represent Dental Pulp Progenitors In Vivo. *J Dent Res*. 2017 Mar;96(3):323-330. doi: 10.1177/0022034516678208. Epub 2016 Nov 13. PMID: 27834664;PMCID: PMC5298392.
41. Wang X, Li X, Zuo X, Liang Z, Ding T, Li K, Ma Y, Li P, Zhu Z, Ju C, Zhang Z, Song Z, Quan H, Zhang J, Hu X, Wang Z. Photobiomodulation inhibits the activation of neurotoxic microglia and astrocytes by inhibiting Lcn2/JAK2-STAT3 crosstalk after spinal cord injury in male rats. *J Neuroinflammation*. 2021 Nov 5;18(1):256. doi: 10.1186/s12974-021-02312-x. PMID: 34740378; PMCID: PMC8571847.
42. Widera D, Zander C, Heidbreder M, Kasperek Y, Noll T, Seitz O, Saldamli B, Sudhoff H, Sader R, Kaltschmidt C, Kaltschmidt B. Adult palatum as a novel source of neural crest-related stem cells. *Stem Cells*. 2009 Aug;27(8):1899-910. doi: 10.1002/stem.104. PMID: 19544446; PMCID: PMC2798069.
43. Wu X, Shen Q, Zhang Z, Zhang D, Gu Y, Xing D. Photoactivation of TGF β /SMAD signaling pathway ameliorates adult hippocampal neurogenesis in Alzheimer's disease model. *Stem Cell Res Ther*. 2021 Jun 11;12(1):345. doi: 10.1186/s13287-021-02399-2. PMID: 34116709;PMCID: PMC8196501.
44. Yang Y, Kim OS, Liu G, Lee BN, Liu D, Fu W, Zhu S, Kang JS, Kim B, Kim O. Effects of Red LED Irradiation in Enhancing the Mineralization of Human Dental Pulp Cells In Vitro. *Int J Mol Sci*. 2023 Jun 5;24(11):9767. doi: 10.3390/ijms24119767. PMID: 37298716; PMCID: PMC10253352.
45. Yoon JH, Choi SH, Koh JT, Lee BN, Chang HS, Hwang IN, Oh WM, Hwang YC. Hard tissueformation after direct pulp capping with osteostatin and MTA *in vivo*. *Restor Dent Endod*. 2021 Feb 25;46(2):e17. doi: 10.5395/rde.2021.46.e17. PMID: 34123753; PMCID: PMC8170379.
46. Ferriello V, Faria MR, Cavalcanti BN. The effects of low-level diode laser treatment and dental pulp-capping materials on the proliferation of L-929 fibroblasts. *J Oral Sci*. 2010 Mar;52(1):33-8. doi: 10.2334/josnusd.52.33. PMID: 20339230.

5. CONSIDERAÇÕES FINAIS

Neste estudo, avaliamos a distribuição de subpopulações de células tronco da polpa dentária, mais especificamente pericitos e células neurais, em diferentes fases de vida, utilizando um modelo animal transgênico com fluorescência endógena. Demonstramos que os pericitos podem estar envolvidos na diferenciação de odontoblastos nos estágios iniciais de formação do dente e em resposta à estímulos nocivos. Por outro lado, as células neurais, uma vez organizadas dentro da polpa dentária se estabelecem como uma fonte adicional de células que parecem contribuir para a manutenção do citoesqueleto da polpa. Observamos também a presença de células nestin no retículo estrelado, uma linhagem epitelial que ainda não havia sido associada a esse marcador.

Além disso utilizamos o mesmo modelo animal, para investigar como a PBMT poderia estimular essas células comparando se essa terapia favoreceria o reparo da polpa dental após um capeamento pulpar com MTA. Demonstramos que a PBMT melhora os resultados do capeamento pulpar com MTA recrutando pericitos tipo II, induzindo a diferenciação de células tronco demonstrada pela expressão de genes de destino odontogênico, produzindo barreira dentinária consistente e reduzindo os sinais inflamatórios quando comparado ao grupo tratado apenas com o MTA.

REFERÊNCIAS

- ABRAHÃO, I. J.; MARTINS, M. D.; KATAYAMA, E.; et al. Collagen analysis in human tooth germ papillae. *Braz Dent J.* v.17, n.3, p.208–212. 2006.
- ALLIOT-LICHT, B; HURTREL, D; GREGOIRE, M. Characterization of alphasmooth muscleactin positive cells in mineralized human dental pulp cultures. *Arch Oral Biol*, v. 46, p. 221-228, 2001.
- ALQADERI, H.; LEE, C.T.; BORZANGY, S.; et al. Coronal pulpotomy for cariously exposed permanent posterior teeth with closed apices: A systematic review and meta-analysis. *Journal of Dentistry*, v.44, p.1–7, 2016.
- ARANY, P.R; CHO, A; HUNT, T.D; et al. Photoactivation of endogenous latent transforming growth factor- β 1 directs dental stem cell differentiation for regeneration. *Sci Transl Med*, v.6, n. 238, p. 238-269, 2014
- BALIC, A.; MINA, M. Characterization of progenitor cells in pulps of murine incisors. *J Dent Res*, v.89, n. 11, 1287-1292, 2010.
- BIRBRAIR, A.; ZHANG, T.; WANG, Z.; et al. Type-1 pericytes participate in fibrous tissue deposition in aged skeletal muscle. *Am Physiol Cell Physiol.* v.305, n.11, p.1098-1113, 2013.
- BIRBRAIR, A.; ZHANG, T.; WANG, Z.; et al. Pericytes at the intersection between tissue regeneration and pathology. *Clinical Science*, v.128 n.2, p. 81-93, 2015.
- CAPLAN, A. All MSCs are pericytes? *Cell Stem Cell*, v. 3, p. 229-230, 2014.
- CUSHLEY, S.; DUNCAN, H.; LAPPIN, M.; et al. Pulpotomy for mature carious teeth with symptoms of irreversible pulpitis: A systematic review. *J Dent.*, v. 88, p. 103158, 2019.
- CUSHLEY, S.; DUNCAN, H.; LAPPIN, M.; et al. Efficacy of direct pulp capping for management of cariously exposed pulps in permanent teeth: a systematic review and meta-analysis. *Int Endod J.*, v. 54, n. 4, p. 556-571, 2021.
- DA COSTA E SILVA, R. M. F.; DINIZ, I. M.; GOMES, N. A.; et al. Equisetum hyemale-derived unprecedented bioactive composite for hard and soft tissues engineering. *Sci Rep.*, v.12, n. 1, p. 13425, 2022.
- DAVAIE, S.; HOOSHMAND, T.; ANSARIFARD, S. Different types of bioceramics as dental pulp capping materials: A systematic review. *Ceram. Int.* v. 47, p. 20781– 20792, 2021.

DELLAVALLE, A.; SAMPAOLESI, M.; TONLORENZI, R.; et al. Pericytes of human skeletal muscle are myogenic precursors distinct from satellite cells. *Nat Cell Biol.*, v. 9, n. 3, p.255-267, 2007.

DES MARAIS D. L.; SMITH, A. R.; BRITTON, D. M.; et al. Phylogenetic relationships and evolution of extant horsetails, *Equisetum*, based on chloroplast DNA sequence data (*rbcL* and *trnLF*). *Int. J. Plant Sci.*, v. 164, p. 737–751, 2003.

DINIZ, I.M.A.; CARREIRA, A. C. O.; SIPERT, C. R.; et al. Photobiomodulation of mesenchymal stem cells encapsulated in an injectable rhBMP4-loaded hydrogel directs hard tissue bioengineering. *J Cell Physiol*, v. 233, n. 6, p. 4907-4918, 2018.

DIDILESCU, A. C.; CRISTACHE, C. M.; ANDREI, M. ; et al. The effect of dental pulp capping materials on hard-tissue barrier formation: A systematic review and metaanalysis. *J Am Dent Assoc.*, v. 149, p. 903–917, 2018.

DORE-DUFFY, P.; MEHEDI, A.; WANG, X.; et al. Immortalized CNS pericytes are quiescent smooth muscle actin-negative and pluripotent. *Microvasc. Res.*, v. 82, p. 18–27, 2011.

DO VALLE, I. B.; PRAZERES, P. H. D. M.; MESQUITA, R. A.; et al. Photobiomodulation drives pericyte mobilization towards skin regeneration. *Scientific Reports*, v. 10, p.19257, 2020.

ELMSMARI, F.; RUIZ, X. F.; MIRO Q.; et al. Outcome of partial pulpotomy in cariously exposed posterior permanent teeth: a systematic review and meta-analysis. *Journal of Endodontics*, v. 45, p. 1296–1306, 2019.

FENG, J.; MANTESO, A.; DE BARI, C.; et al. Dual origin of mesenchymal stem cells contributing to organ growth and repair. *Proc Natl Acad Sci U S A.*, v. 108, p. 6503–6508, 2011.

GOMES, N. A.; DO VALLE, I. B, GLEBER-NETTO, F. O.; et al. Nestin and NG2 transgenes reveal two populations of perivascular cells stimulated by photobiomodulation. *J Cell Physiol.*, v. 237, n. 4, 2198-2210.

KAUKUA, N.; SHAHIDI, M. K.; KONSTANTINIDOU, C.; et al. Glial Origin of Mesenchymal Stem Cells in a Tooth Model System. *Nature*, v. 513, n. 7519, p. 551-554, 2014.

KYYRIAINEN, J.; ENDODE-EKANE, E.; XAVIER, P. A. Dynamics of PDGFR β Expression in Different Cell Types After Brain Injury. *Glia*, v. 65, n. 2, p. 322-341, 2017.

LØVSCHELL, H.; GIANNOBILE, W.; SOMERMAN, M.; et al. Stem cells and

regeneration of injured dental tissue. In: Textbook and Color Atlas of Traumatic Injuries to the Teeth. 2007.

MANCINELLA, A. Silicon, a trace element essential for living organisms. Recent knowledge on its preventive role in atherosclerotic process, aging and neoplasms. Clin. Ter, v. 137, p. 343– 350, 1991.

MARCHESAN, J.; GIRNARY, M. S.; JING, L.; et al. An experimental murine model to study periodontitis. Nature Protocols., v. 13, p. 2247–2267, 2018.

MIHAELA, C.; SOLOMON, Y.; LOUIS, C.; et al. A perivascular origin for mesenchymal stem cells in multiple human organs. Cell Stem Cell., v.11, n.3, p. 301- 313, 2008.

MOREIRA, M. S.; DINIZ, I. M. A.; RODRIGUES, M. F. S. D.; et al. In vivo experimental model of orthotopic dental pulp regeneration under the influence of photobiomodulation therapy. J Photochem Photobiol B, v. 166, p. 180-186, 2017.

NEHLS, V.; DRENCKHAHN, DETLEV. The versatility of microvascular pericytes: From mesenchyme to smooth muscle? Histochemistry, v. 99, n. 1, p. 1-12, 1993.

JONES, J. R.; EHRENFRIED, L. M.; HENCH, L. L. Optimising bioactive glass scaffolds for bone tissue engineering. Biomaterials, v. 27, p. 964–973, 2006.

SAMPAIO, I. B. M. Estatística Aplicada à Experimentação Animal. 3. ed. Belo Horizonte: Fepmvz; 2007.

SÁ-PEREIRA, I.; BRITES, D.; BRITO, M. A. Neurovascular unit: a focus on pericytes. Mol Neurobiol, v. 45, n. 2, p.327-347, 2012.

SHI, S.; GRONTHOS, S. Perivascular-Derived Mesenchymal Stem Cells. J Dent Res., v. 98, n. 10, p.1066-1072, 2019.

SHIH, S. J.; CHOU, YU. JEN.; CHIEN, I.C. One-step synthesis of bioactive glass by spray pyrolysis. J Nanopart Res., p.14. 2012.

VIDOVIC-ZDRILIC, I.; VINING, K. H.; VIJAYKUMAR, A.; et al. FGF2 enhances odontoblast differentiation by α SMA+ progenitors in vivo. Journal of Dental Research, v. 97, p. 1170–1177, 2018.

VIDOVIC, I.; BANERJEE, A.; FATAHI, R.; et al. SMA- expressing perivascular cells represent dental pulp progenitors in vivo. Journal of Dental Research.

YIANI, V.; SHARPE, P. T. Perivascular-Derived Mesenchymal Stem Cells. J Dent Res, v. 98, n. 10, p. 1066-1072, 2019.

ZIMERMANN, K.W. Der feinere Bau der Blutkapillaren. Z. Anat. Entwicklungsgesch, v. 68, p. 29–109, 1923.

ANEXO



UNIVERSIDADE FEDERAL DE MINAS GERAIS

CEUA
COMISSÃO DE ÉTICA NO USO DE ANIMAIS

Prezado(a):

Esta é uma mensagem automática do sistema Solicite CEUA que indica mudança na situação de uma solicitação.

Protocolo CEUA: 181/2021**Título do projeto:** ESTUDO SOBRE A FOTOBIMODULAÇÃO DE PERICITOS EM INJÚRIA DA POLPA DENTÁRIA IN VIVO - Uma Continuação**Finalidade:** Pesquisa**Pesquisador responsável:** Ivana Marcia Alves Diniz**Unidade:** Faculdade de Odontologia**Departamento:** Departamento de Odontologia Restauradora**Situação atual:** *Decisão Final - Aprovado*Aprovado na reunião ordinária on-line do dia 13/09/2021. Validade: 13/09/2021 à 12/09/2026.
Belo Horizonte, 13/09/2021.

Atenciosamente,

Sistema Solicite CEUA UFMG

https://aplicativos.ufmg.br/solicite_ceua/Universidade Federal de Minas Gerais
Avenida Antônio Carlos, 6627 – Campus Pampulha
Unidade Administrativa II – 2º Andar, Sala 2005
31270-901 – Belo Horizonte, MG – Brasil
Telefone: (31) 3409-4516
www.ufmg.br/bioetica/ceua - cetea@prpq.ufmg.br